

THE EFFECT OF WEATHERING ON THE FLAMMABILITY OF A SLICK OF CRUDE OIL ON A WATER BED

Neil Wu (*), Gilles Kolb() and Jose L. Torero (***)**

Department of Fire Protection Engineering
University of Maryland
College Park, MD20742-3031
USA

(*) Present Address:

Rolf Jensen & Associates, Inc.
5850 T.G. Lee Blvd.Suite 650
Orlando, FL 32822-4407, USA

() Present Address:**

Royal Institute of Technology
Division of Nuclear Power Safety
Brinellvägen 60
100 44 Stockholm, Sweden

(*) Corresponding Author:**

Department of Fire Protection Engineering
University of Maryland
College Park, MD20742-3031
USA
e-mail: J.Torero@ed.ac.uk

ABSTRACT

An experimental study to define a practical methodology that will serve to assess the burning of crude oils on a water sub-layer by means of a bench scale procedure is presented. A modified ASTM-E1321 (LIFT) is combined with flash point measurements to extract fuel properties by means of an existing theoretical formulation. The fuel and water layers are treated as a thermally thick material with combined properties to be able to obtain an analytical solution for an ignition delay time and a flame spread velocity. The experimental results are then correlated to the theoretical formulation to obtain the “fire properties” described in the ASTM-E1321 standard. Five different parameters have been identified that describe the capability of a liquid fuel to sustain a flame: the critical heat flux for ignition, $\dot{q}_{0,ig}''$, an ignition temperature, T_{ig} , the heat contribution of the flame, ϕ , a thermal efficiency, a/h_T and the thermal inertia, $\sqrt{k\rho c}/a$. The methodology is used to evaluate the effect of weathering on the flammability of Alaska North Slope (ANS) and Cook Inlet crude oils. The critical heat flux for ignition was found to be a strong function of the weathering level and a weak function of the fuel layer thickness. The ignition temperature depends on both the weathering level and the fuel layer thickness. Thermal efficiency, heat contribution from the flame and thermal inertia remained invariant with the weathering level and fuel layer thickness.

INTRODUCTION

Burning of an oil spill is of interest as a result of offshore exploration, production, and transportation of petroleum (Koseki et al., 1991). Sensitive oceanic environments require immediate response to remove a hazardous oil slick. In-situ burning can be an effective response tool for a fast removal of an oil slick to minimize the negative environmental impact. Cleanup by combustion can be, in certain specific conditions, a more attractive counter-measure than other spill mitigation methods. This approach requires less labor than other removal techniques, such as using mechanical recovery or chemical dispersants. Furthermore, the efficiency of in-situ burning, 85 – 99%, is greater than mechanical recovery or dispersant efficiency, 33 – 67% and 50 – 70%, respectively (Tebau, 1994, Walavalkar and Kulkarni, 1996)). Primarily, in-situ burning is employed to rapidly remove a large volume of oil from the surface of water to reduce subsequent environmental effects.

Although in-situ burning is relatively simple, effectiveness is limited by various physical factors, such as oil slick thickness, degree of weathering, amount of emulsification, and environmental conditions. Generally, quicker response by in-situ burning results in a higher efficiency. Thickness of the slick affects the burning of a crude oil. For instance, an oil slick continues to burn until it reaches a minimum thickness range between 0.8mm to 3mm (Kennedy et al., 1994). When the oil slick goes below this level, heat loss to the water underneath is sufficient to quench the fire. Since an oil slick tends to disperse and spread with time, more effective burning is achieved by quicker response.

Most accidental and deliberate burns of spilled oil at sea suffer from the effects of wind and waves. Spreading and evaporation can alter the characteristics of an oil slick. Volatiles tend to evaporate rapidly with time (weathering) and mixing tend to form oil/water emulsions making

the oil difficult to ignite. Consequently, alteration of the physical or chemical properties of the oil can require additional energy for ignition. Several studies have attempted to characterize weathering and emulsions typical of oil-spill scenarios (Bobra, 1992).

Though vast studies exist on the operational implications (applicability, cost, environmental damage, human health concerns) of in-situ burning, actual burning characteristics, such as ignition and flame spread data, is limited. Thus, further experimentation is necessary to analyze the limitations of in-situ burning and to characterize the potential of different fuels, or oil spill scenarios, to be treated by means of this response method.

In-situ burning of an oil spill is accomplished through three distinct stages of combustion; (1) ignition, (2) flame spread, and (3) self-sustained burning (or more commonly mass burning). An external source of energy will ignite the liquid fuel and, under ideal conditions, will be followed by the spread of a flame over the surface of the fuel. Once the flame spread process is self-sustained, mass burning will follow. Many studies have shown that ignition is not always followed by spread (Kashiwagi et al., 1997) therefore, is not sufficient to guarantee efficient removal of the oil slick.

Information available on burning of a thin fuel layer floating on a water sub-layer is quite limited. Walavalkar and Kulkarni (1996) compiled an extensive review of studies involving ignition, flame spread, and mass burning of crude oils. However, this review focuses primarily on the burning efficiency of crude oil emulsions, in which success is measured solely by the fraction of the spilled oil that is burned away. The authors further indicate there is a lack of fundamental studies to understand the basic mechanisms of crude oil combustion.

Crude oils are generally complex in composition with multiple hydrocarbon components. Although ignition behavior of individual petroleum fractions has been studied using flash and

fire points under quiescent conditions (Glassman and Dryer, 1980, Ross, 1994, SFPE, 1994), complete multi-component crude oils has not been addressed either in the virgin or weathered states. The influence of weathering and the formation of oil/water emulsions on the flash and fire points have yet to be studied. To the knowledge of the authors, the only study that addresses the effect of weathering and formation of emulsions on ignition under conditions pertinent to the oil-spill scenario is that of Putorti et al. (1994). This study was conducted using a cone calorimeter and quantified the necessary heat flux for ignition of various liquid fuels. In this work, emphasis was placed on the ignition delay time of weathered and emulsified samples.

Flash and fire point temperatures have been commonly used as single criteria in the evaluation of the “flammability” of liquid fuels, although, many studies (Glassman and Dryer, 1980) have shown that flash/fire point temperatures are not sufficient criteria to determine the conditions necessary for a liquid fuel to sustain or propagate a flame. Furthermore, for this particular application, the presence of a water bed adds one more parameter that requires in-depth evaluation.

Flash or fire point tests do not incorporate the effects that high heat insult has on the nature of the fuel, i.e. emulsions break down when subject to a high heat flux, thus are insufficient when describing an oil spill scenario. Furthermore, heat transfer towards the water sub-layer is entirely dependent on the fuel properties and can preclude ignition. Under certain conditions, the water sub-layer starts to boil, penetrates the fuel layer, and ejects water droplets to the surroundings. This phenomenon is caused by thermal penetration of the heat wave reaching the fuel-water interface and is termed “thin layer boilover” (Arai et al., 1990, Garo et al., 1994, Koseki et al., 1991). Thin-layer boil-over has been found generally to enhance burning rate although Koseki et al. (1991) noted that boiling at the fuel-water interface can limit flame spread. The effect of

minimum fuel layer thickness necessary for sustained combustion has been studied extensively (Arai et al., 1990, Garo et al., 1994). Several models have been developed to describe the heat losses from a pool fire to the supporting water layer (Brzustowski and Twardus, 1982) and to attempt description of in-depth absorption of radiation by the fuel layer (Twardus and Brzustowski, 1981).

Flame spread over a liquid has been shown to be a complex phenomenon that can not be fully described, in contrast with solid fuels, by means of a heat transfer analysis. Glassman and Dryer (1980), Sirignano and Glassman (1970), and more recently Ross (1994), have shown that flow structures formed ahead of the flame front due to capillary motion and buoyancy affect significantly the flame spread rate. Infra red thermography has been used by Inamura et al. (1992) to show the enhanced heat transfer due to convective motion in the fuel bed. Many other studies, reviewed by Glassman and Dryer (1980) and Ross (1994), have described the different controlling mechanisms of flame spread over liquid fuels. Nevertheless, studies that emphasize the role of weathering or a water substrate on flame spread are scarce.

In contrast, mass burning has been studied extensively and Mudan and Croce (1994) provide a comprehensive review. Burning efficiency under conditions relevant to this study has been presented elsewhere (Garo et al., 1996, Garo et al., 1999), therefore this subject will not be addressed here.

Knowledge on ignition, spread and burning rate can contribute to the determination of adequate flammability criteria for crude oils under conditions relevant to an oil-spill. Material flammability of liquid and solid fuels has been researched extensively. Recognised testing standards containing strict testing protocols are currently available to facilitate material fuel properties (ASTM, 1990, ASTM, 1994).

Determination of flammability criteria is necessary to improve ignition protocols and to enhance efficiency during in-situ burning of oil spills. The present work concentrates on the ignition and flame spread characteristics and aims to provide information that will help defining ignition protocols. In this work, two combined standard methodologies, ASTM-E-1321 (LIFT Test) (ASTM, 1994) and ASTM-D56 (Closed Cup Flash Point Test) (ASTM, 1990) are used to determine a series of properties that provide a more detailed evaluation of the flammability of a crude oil in conditions typical of an oil-spill scenario.

EXPERIMENTAL APPROACH

The Lateral Ignition and Flame Spread Test

Generalities

The Lateral Ignition and Flame Spread Test, or LIFT standard has been developed to quantify material properties of combustible solids in a small-scale test. Material properties related to piloted ignition of a vertically orientated sample under a constant and uniform heat flux and to lateral flame spread on a vertical surface due to an external radiant flux, are obtained through this testing standard. The LIFT has the advantage that it allows for ignition and flame spread to be studied together which provides a more realistic scenario than other test methods. The background behind this test method is supported by a well-documented theoretical foundation (ASTM, 1994, Quintiere, 1981, Quintiere et al, 1983, Quintiere and Harkleroad, 1984). Therefore, it provides an adequate framework for the study of complex fuels.

The LIFT test has two distinct procedures, one for piloted ignition and the other for flame spread. Piloted ignition is conducted with a constant external heat flux and flame spread with a decaying one. The material properties of the fuel can be extracted from this information. Results from the ignition portion of the LIFT standard provide an effective material thermal inertia ($k\rho C$), a minimum surface flux and temperature necessary for ignition ($\dot{q}''_{o,ig}$ and T_{ig}). From the lateral flame spread test, the minimum flux necessary for sustained flame propagation ($\dot{q}''_{o,s}$), the minimum temperature required for flame spread ($T_{s,min}$), and a flame-heating parameter (ϕ) which is dependent on test conditions, such as the opposed flow gas velocity, the ambient oxidizer concentration, and the properties of the fuel (Quintiere and Harkleroad, 1984).

Together, these specific properties can be used to classify materials based on their ignition and flame spread behavior.

The basis of the theoretical model behind the LIFT can be described as piloted ignition and flame spread as a result of inert heating of a thermally thick homogeneous solid to an ignition temperature. The flame configuration applies to a flame spreading into an opposed ambient flow, which closely simulates the flame spread occurring in in-situ burning.

Details on the LIFT hardware, testing protocol and theoretical underpinnings have been extensively documented by Quintiere and co-workers (Quintiere, 1981, Quintiere et al., 1983 and Quintiere and Harkleroad, 1984) and therefore will not be detailed here.

Modification of the L.I.F.T. Apparatus

The ASTM E1321 experimental apparatus has been used to study the ignition and flame spread characteristics of liquid fuels on a supporting bed of water. The L.I.F.T. hardware had to be significantly modified for this purpose. Figure 1 shows a schematic of the modified hardware. Since both the panel and sample-holder apparatus are rotated 90° to the horizontal configuration, the modified hardware is commonly referred as H.I.F.T. (Horizontal Ignition and Flame Spread Test). Previously, this geometrical configuration has been used to study materials from which the vertical configuration was not convenient (Motevalli et al., 1992). The configuration is similar to the LIFT apparatus, however, the experimental HIFT apparatus contains six major modifications. The modified elements are the following: (1) an induced flow; (2) a radiation shield; (3) sample holders; (4) a pilot flame; (5) a data acquisition system; and (6) the radiant panel. Additionally, revised procedures are required for use of the modified apparatus.

An electric powered fan 4 inches in diameter is used to induce a draft to establish a well-defined fuel boundary layer. The flow-generating device is placed 50 mm from the trailing edge of the sample. Additionally, a metal duct is used to develop a flow parallel to the fuel surface. The duct shown in Figure 1 has a 200mm square cross section which contains an 80mm thick bed of packed steel wool located at the end nearest to the sample. The steel wool serves to homogenize the induced flow creating a constant laminar flow of 0.1 m/s for at least the 100 mm region over the ignition tray surface.

A calcium silicate board of 10mm thickness is used as a radiation shield to prevent premature heating of the sample. The shield is positioned above the sample and extends beyond the length of the entire flame spread tray (500mm). A roller-based system is used to facilitate movement of the radiation shield. Rollers are attached to the frame of the shielding device for rapid removal and replacement.

All sample holders are constructed from bare 1.2 mm thick stainless steel. The ignition and flame spread specimen holders are reduced in size compared to the original LIFT equipment to 100 mm square and 100 by 500mm, respectively. Although studies have shown that viscous effects are only negligible for fuel pans greater than 200 mm (Glassman and Dryer, 1980), the presence of the radiant panel precluded the use of a larger tray. The use of larger tray required a larger panel (edge effects) and results in larger flames and a significant increase in radiative feedback. For the purposes of this work, it is important to minimize radiative feedback from the flames since it can not be isolated from the external radiation provided by the panel. Glassman and Dryer (1980) showed a 15~20% increase in the propagation velocity between 100 mm and 200 mm width trays, independent of radiative feedback. Thus, the flame spread velocities

reported in this work will be slower than those corresponding to a larger pan and this difference will be considered part of the experimental error.

Figure 2 shows the dimensions of the ignition tray used for experimentation. Additionally, a 250 mm x 250 mm aluminum plate (1.2mm thickness) is placed around the ignition sample to simulate a floor around the liquid pool. A hole measuring to the exact dimensions of the ignition tray is removed from the center of the plate. A thermocouple tree is placed on the side of the tray (Figure 2) with the thermocouple tips positioned in the axis of symmetry of the tray. No correction for radiation will be performed for the measurements.

Figure 3 shows a schematic of the experimental tray used in the flame spread tests. Ten thermocouple identical to those used in the ignition tests are placed down the center plane of the flame spread tray. Heights are adjusted to position the thermocouples at the surface of the liquid fuel. Considerations for fuel expansion are taken, but the inherent limitation of this technique is the accurate positioning of the thermocouple tip. Both flame spread and ignition trays are transported to the testing position by a precision metal roller and track system.

A propane diffusion flame is provided to ensure piloted ignition of the sample. A small propane diffusion flame (20 mm in height) established on a 4 mm stainless-steel nozzle was used as an ignition pilot. Pilot location and height is fully adjustable. Flame height is varied by regulating the propane gas flow. As illustrated in Figure 2, the pilot flame was positioned 10 mm above the fuel surface in the centerline 10 mm downstream of the trailing edge of the ignition tray. Size and location of the pilot were a subject of a systematic study, and the final positioning was chosen to maximize repeatability of the results and to minimize heat feedback from the pilot flame to the surface. This issue has been addressed previously by Glassman and

Dryer (Glassman and Dryer, 1980) who showed that heat feedback from the pilot flame can significantly alter ignition and spread.

The data acquisition system software is a PC/Windows-based program by Labtech (Release 9). Measurement devices are Omega Type K stainless steel sheathed thermocouples with a diameter of 0.8mm. The thermocouples are attached to an Omega EXP-32 external input board. The system allows for 32 input channels with a scan frequency of 1 Hz. Furthermore, the system can be initiated either manually or automatically using the data acquisition software.

Video recordings of all tests were made with a Sony 8 mm video camera. The video camera records allow determination of the ignition event precisely and simultaneously register the time and position of the flame front on the fuel surface. Graduated markings are used along the length of the tray.

The radiant panel and sample orientation are rotated 90° to the horizontal axis. Other than orientation, the radiant panel design and operation is unaltered from the ASTM standard. Although distance of the radiant panel is lengthened to increase the sensitivity of radiant exposure to a lower range of heat fluxes than that commonly used for solid materials, inclination of the panel remains at 15°. Initially, the panel was calibrated according to the ASTM E1321 standard protocol. As described in detail by the standard, the gas-fired radiant panel should emit a uniform heat flux over the length of the ignition sample. Calibration of incident heat flux results is shown in Figure 4. Over the length of the ignition sample holder, the incident heat flux is $\pm 6\%$ of the nominal value followed by a heat flux distribution that decreases in the stream wise direction. For ignition and spread tests, the nominal value referred to in the text as \dot{q}_i'' will be the peak heat flux.

Although the ASTM E1321 apparatus is well characterized, modification into the HIFT apparatus generates important testing complexities. To study these small-scale testing phenomena, a series of tests were conducted using SAE 30-Weight oil. Selection of the SAE 30W oil is not arbitrary; the increased flash point temperature (254°C) allows for longer observation times during testing. Topics addressed during these are (1) the effect of the container geometry, (2) the effect of a flush floor surrounding the ignition sample, (3) the effect of an induced draft, and (4) the effect of pilot position on ignition delay time. Details of this evaluation can be found in Wu et al. (1996 and 1998) and will not be repeated here. It was concluded that a stable laminar flow is necessary, both to eliminate the need to keep the pilot flame over the fuel surface and to create a robust flow structure that can be considered independent of the environment. The use of the floor and parallel flow was justified on the basis of producing a homogeneous flow structure and avoiding any re-circulation zones, possibly present at the leading edge close to the fuel surface. In summary, these studies provide a rigorous protocol that allows for best repeatability and to set the test conditions to reproduce at best the theoretical assumptions used.

Closed Cup Flash Point Test

The ASTM D56 Tag Closed Cup flash point tester was used to characterize the thermal properties under a controlled environment. The standard should be referenced for details of the apparatus (ASTM-Fire Test Standards, 1990). Flash point is defined as the lowest temperature corrected to a pressure of 760 mm Hg at which application of a test flame causes the vapor of a portion of the sample to ignite under specified conditions. The flash point measures the tendency of a fuel to form a combustible mixture with air under a controlled laboratory condition. It is

only one of a number of properties that must be considered in assessing the overall thermal characteristics of a liquid fuel.

For the test for a flash point, a liquid fuel is placed in the cup of the tester. With the lid closed, the sample is heated up at a slow constant rate. A small flame of specified size is directed into the cup at regular intervals. The lowest temperature at which application of the flame ignites the vapors above the sample specifies the flash point. The flash point temperature gives an indication of the pyrolysis temperature of the fuel but not of the thermal properties that will lead to the attainment of this temperature. Therefore, the flash point temperature is of importance but not sufficient to describe the ignition process.

Weathering

Evaporation is the dominant weathering process that affects the crude oils in the marine environment. Depending on the conditions, the physical, chemical, and toxicological properties of a crude oil can be altered significantly by evaporation. The changes induced by evaporation will have a determinant effect on in-situ burning, since they will affect ignition (Putorti et al., 1994) and most probable, flame spread and mass burning. Therefore, characterization of the weathering process is of importance to the application of the overall testing methodology.

Few references are available that provide sound results relating accelerated laboratory evaporation of crude oils to actual field conditions, this work does not attempt to provide further insight in this area but to simply quantify the evaporation by mass loss, which is sufficient for characterization of the crude oil combustion.

Hydrocarbons constitute the most important fraction in any crude oil. Although the proportions of each fraction varies significantly, (e.g. from 30-40% to 100% in gas condensates), they account for up to 70% in all petroleum on the average (Petrov, 1987). The light boiling

fractions of standard crude oil can contain up to 150 different hydrocarbons. The complexity of petroleum hydrocarbon makes identification of individual elements difficult. The development of gas chromatography-mass spectrometry allowed classification of fractions of individual groups according to molecular structure: (1) Alkenes (C_5 - C_{40}); (2) Napthenes or Cycloalkenes; and (3) Aromatic Hydrocarbons (Arenes).

The least complicated are the Alkenes, which are divided into three fractions. Fraction I is of primary interest since the C_5 - C_{11} hydrocarbons are distilled from the crude oil at a temperature range of 30-200 °C, which corresponds to almost the entire range of interest. McAuliffe (1989) characterized evaporation as a function of time to liberate the C_9 and lower hydrocarbons. Similarly, the Bartlesville Project Office (BPO) Crude Oil Analysis Data Base User's Guide specifies the C_8 fraction (light gasoline) to be distilled at temperatures of 100°C (Sellers et al. (1996)). The selection of this criteria is not arbitrary as the lighter fractions were not only the most likely to evaporate, but also the most biologically hazardous. This is the referencing standard to compare accelerated laboratory weathering to field conditions. Therefore, an analysis of only simple unsaturated hydrocarbons ($<C_{11}$) is made between individual petroleum fractions and weathered Cook Inlet and ANS crude oils. Complicated components such as saturated cyclic hydrocarbons (naphthenes) and aromatic hydrocarbons have been omitted because of the complex nature of these fractions.

As mentioned previously, data correlating accelerated laboratory evaporation to weathering in a marine environment is relatively limited. One particular computational model, EUROSPILL, was developed to provide information on the chemical release of hydrocarbons from a slick of oil to the atmosphere and water (Rusin et al., 1996). Data extracted from several laboratory experiments were used as inputs for the spill algorithm. For tests conducted using

pure styrene and divinylbenzene on open water with winds of 10 knots and 0.9 meter high waves, the model accurately predicted the rate of evaporation. In a similar effort, Reijnart and Rose (1982) investigated the effects of temperature, mixing, wind, and slick thickness on the rate of evaporation. Batch evaporation experiments with Ekofisk, Brent, Kuwait, and Burgan crude oils correlated very well with their evaporation model. Although simulating controlled field conditions was difficult, predicted evaporation by their model was in good agreement with full-scale sea spills.

Finally, Ostazeski et al. (1996) provide a detailed study of the weathering properties and the predicted behavior at sea of a No. 6 fuel oil. Because of the similarities to crude oil, No. 6 fuel oil was artificially weathered in a laboratory and used as inputs to the IKU Oil weathering model. Although large-scale experiments were not conducted to validate this predictive evaporation model, a mass loss of 10-20% by weight is predicted after 5 days with a sea surface temperature of 20°C. A similar evaporation trend is expected from both Cook Inlet and ANS crude oils and therefore these reference values will be used to determine the upper evaporation threshold for these experiments.

Description of the Laboratory Weathering Station

Weathering is simulated in the laboratory using an Arrow Engineering, Inc. Model 493SG rotary evaporator. Using this method of evaporation, time, temperature, volume and mixing velocity can be controlled to produce exposures that will result in a mass loss of comparable magnitude to those observed in the first days of an oil-spill. Temperature of the sample is controlled by using a thermostatically controlled water bath, and mixing velocity is regulated by controlling the input air pressure of the pneumatic rotary evaporator. The rotary evaporator has three different velocity settings, no rotation (will be labeled “none”),

approximately 60 r.p.m. (will be labeled “half”) and approximately 120 r.p.m. (will be labeled “full”). Weathering is measured on a mass loss basis using an Acculab Model V-1200 digital scale with an accuracy of $\pm 0.05\text{g}$.

Characterization of the Weathered Fuels

The following section illustrates the effect of varying the volume, mixing and temperature conditions. The data is presented as a percentage mass loss that was obtained from the ratio between the mass lost after a certain specific period and the initial mass of the sample. The values presented are averages of at least four different tests. Results obtained in this study are in good agreement with all known sources of laboratory crude oil evaporation.

The Effect of the Initial Volume and Mixing

It has been observed during oil-spills that evaporation starts at the surface of the fuel and penetrates with time, thus fuel layer thickness has a significant effect on the weathering process. In a laboratory scale it is necessary to obtain homogeneously evaporated oil, therefore mixing is introduced to guarantee this homogeneity. The initial volume of the fuel sample influences the effectiveness of mixing, therefore, these parameters were varied systematically and the total mass loss recorded. Experiments were conducted with Cook Inlet and ANS crude oils for a variety of conditions, but for brevity only representative cases will be presented to explain the trends. A complete set of results can be found in Wu (1998).

The initial volume of the sample was increased keeping all other parameters invariant while the mass loss was recorded, the results are presented in Figure 5. This figure shows that an increase in the volume of fuel reduces the evaporation rate. This dependency is expected since the global mass loss rate is a function of the surface to volume ratio. Similar trends are noticed for the evaporation of ANS crude oil as a function of initial volume (Wu (1998)). It needs to be

noted that for all the data presented in Figure 5 a rotary evaporator was set to an intermediate velocity.

Mass loss data was taken for different velocities of the rotary evaporator. When mixing is introduced evaporation occurred faster (Figures 6), independent of the speed of the rotor. Enhancement of the evaporation rate due to mixing occurred for a very low rotor speed, and it was impossible to determine the speed at which the transition between the slow and fast evaporation rate occurred. This limitation was imposed by the discrete number of speeds of the rotary evaporator used for the present study. As mentioned before, larger volume results in a slower evaporation rate. Figure 6 shows data for two different volumes and various rotator velocities for Cook Inlet crude oil. The data presented shows that the characteristic time for evaporation is much larger than the characteristic flow time introduced by the rotary evaporator, which guarantees a homogeneous mixture.

The Effect of Temperature

To study the effects of temperature on the rate evaporation, all other parameters were held constant and mass loss was recorded. To ensure the temperature of the crude oil remained constant through the test duration, the automated thermostatic control specified previously was used, typical results for Cook Inlet crude oil are presented in Figure 7. This plot shows that an increase in temperature results in an increased evaporation rate. Therefore, a larger percentage of fuels evaporate for a specified time period. Furthermore, Figure 7 illustrates an almost linear dependency of the mass loss with temperature. Similar results were obtained with ANS crude oil.

A linear dependency of the mass loss with temperature has been previously reported by Fingas (1996) who also provides logarithmic curve fits for the time evolution of the mass loss.

The present results correspond well with this work. No attempt of making such a correlation will be made here since a detailed characterization of the evaporation process goes beyond the scope of this work.

Bobra (1992) takes a similar approach to Fingas (1996) to describe experiments conducted with ANS and other common crude oils but also varies the initial fuel volume. The results also show a logarithmic relation of mass loss over time using a rotary evaporator and identical decrease in evaporation with an increase in volume. This logarithmic trend is physically representative of the additional effort required to volatilize the heavier remaining crude fractions. However, in the study conducted by Bobra, the evaporation time was extended to an order of magnitude of a week, which resulted in mass losses of 30-40% for ANS. Due to safety precautions, and based on the conclusions of Ostazeski et al. (1996) evaporation tests for this study were limited to 8 hours producing approximately 20% weight loss of ANS crude and 25% for Cook Inlet oil.

Methodology

Selection of the weathering method (temperature, rotator velocity, and initial volume) is based upon three criteria: (1) time; (2) accuracy; (3) and repeatability. Therefore, from the data presented above, it is justified that a minimum initial volume of 600mL, the “half” rotator velocity setting, and a temperature of 85°C are used. The “half” setting is selected in preference to the “full” setting because the latter resulted in slight mass loss due to splashing, which subsequently leads to a larger experimental error. These settings allow for accurate, repeatable tests that minimize the time to reach the desired mass loss goal. The percent mass loss will be used as a reference parameter for the level of weathering. No attempt to correlate this value with actual oil spill scenarios will be presented.

THEORETICAL BACKGROUND

Introduction

To analyze a fuel layer floated on water, the fuel and water layers are assumed as one thermally thick bed with properties corresponding to an unknown combination of both liquids. Furthermore, the bed is assumed a semi-infinite slab. Thus, all convective and thermo-capillary motion in the bed is neglected. This assumption is not necessarily correct (Glassman and Dryer, 1980 and Ross , 1994), especially for a small scale where the possibility of temperature gradients between the tray and the liquids is significant. Wu et al. (1998) discussed in detail this issue for the specific configuration used for this study and showed that although these re-circulation currents were present, had a small effect on the ignition results. The effect on flame spread results will be addressed in following sections.

The liquid bed is considered initially at a constant ambient temperature, T_i . Throughout the pre-heating process the fuel layer is assumed inert with negligible pyrolysis before ignition.

The solution to the one-dimensional transient heating of a semi-infinite slab is given by Carslaw and Jaeger (1963) and used by Quintiere (1981) as the starting point of the ignition and flame spread analysis. A brief summary of this analysis will be presented here, details can be found in the work of Quintiere (1981).

Ignition

The mechanisms leading to gas phase ignition from a condensed fuel can be described as follows. The solid fuel sample is considered initially at ambient temperature, T_∞ . After suddenly imposing an incident heat flux (\dot{q}_i''), the temperature of the solid fuel sample rises until the surface reaches the temperature at which the fuel first produces volatiles, this will be referred as the vaporization temperature (T_v). The time required for the fuel surface to attain T_v will be

referred the vaporization time, t_v . After attaining T_v , increasing amounts of vapor leaves the surface, is diffused and convected outwards, mixes with the ambient oxidizer, and creates a flammable mixture near the solid surface. This period will be referred here as the flammable mixture time (t_m). A small temperature increase at the surface, which relates mostly to pyrolysis kinetics, can be observed throughout this period. The fuel properties, flow and geometrical characteristics determine the flammable mixture time and a characteristic surface temperature, T_m , at the end of this period. At this point, the ignition process relates only to the gas phase. If the mixture temperature is increased the combustion reaction between the fuel vapor and the oxidizer gas may become strong enough to overcome the heat losses, thus becoming self-sustained, at which point flaming ignition will occur. This period corresponds to the induction time (t_i) and is characterized by a gas phase ignition temperature (T_i). Induction time and ignition temperature are derived from a complex combination of fuel properties and flow characteristics.

Extending the analysis proposed by Fernandez-Pello (1995), the ignition delay time (t_{ig}) can be given by

$$t_{ig} = t_v + t_m + t_i \quad (1)$$

Introducing a pilot reduces the induction time (t_i) making it negligible when compared to t_v and t_m . Furthermore, the period where the transient evolution of the fuel concentration in the gas phase increases towards a flammable mixture (t_m) has been commonly considered short when compared to heating of the solid fuel sample. The magnitude of the induced forced flow (0.1 m/s) was established to guarantee that $t_m \ll t_v$. In the L.I.F.T. the sample is placed vertically, therefore, natural convection will induce flows of similar magnitude. Under these conditions the fuel and oxidizer mixture can be considered to become flammable almost immediately after

vaporization starts. Vaporization temperatures and times are thus commonly referred to as ignition temperature (T_{ig}) and ignition delay time (t_{ig}) (Quintiere, 1981) and equation (1) simplifies to $t_{ig} = t_v$ and T_{ig} can be defined as T_v .

Ignition Delay Time (t_{ig})

The energy balance at the surface of the fuel under radiative heating is given by equation (2).

$$\dot{q}_s''(0, t) = a \dot{q}_i'' - \varepsilon \sigma (T^4(0, t) - T_\infty^4) - h_c (T(0, t) - T_\infty) \quad (2)$$

Where (\dot{q}_s'') is the net heat flux at the surface of the solid fuel sample, (\dot{q}_i'') the imposed external heat flux, (a) is the absorptivity of the fuel, (ε) is the emissivity of the fuel, (σ) is the Stefan-Boltzmann constant, ($T(0, t)$) is the surface temperature at time (t), (h_c) is the convective heat transfer coefficient, and (T_∞) is the ambient temperature.

To obtain an analytical solution Quintiere (1981) assumes a linear approximation for the surface re-radiation. The radiative term is then defined as:

$$\varepsilon \sigma (T^4(0, t) - T_\infty^4) = h_r (T(0, t) - T_\infty) \quad (3)$$

Controversy on the effect of this approximation on the determination of the minimum heat flux necessary to attain the ignition temperature is still unresolved. Due to the complexity of the fuels studied in the present work, concentration will be given to the use of this methodology, therefore this issue, although of great importance, will not be addressed here.

Substituting (3) into (2) and assuming that the total heat transfer coefficient (h_T) is equal to the sum of the convective heat transfer coefficient (h_c) and the radiative heat transfer coefficient (h_r), the following expression (4) defines the net heat flux (\dot{q}_s'') at the surface of the solid fuel sample.

$$\dot{q}_s''(0, t) = a \dot{q}_i'' - h_T (T(0, t) - T_\infty) \quad (4)$$

The differential formulation of the governing energy equation is given by:

B.C.

$$\frac{\partial^2 T}{\partial x^2} = \frac{1}{\alpha} \frac{\partial T}{\partial t} \quad x = 0, -k \frac{\partial T}{\partial x} = \dot{q}_s''(0, t) \quad (5)$$

$$\begin{aligned} t &= 0 & T &= T_\infty \\ x &\rightarrow \infty \end{aligned}$$

by means of a Laplace transformation, a general solution for the temperature at the surface (T_s), can be obtained:

$$T_s = T_\infty + \bar{T} \left[1 - e^{t/t_c} \operatorname{erfc} \left(\left(\frac{t}{t_c} \right)^{1/2} \right) \right] \quad (6)$$

where

$$\bar{T} = \frac{a \dot{q}_i''}{(h_T)}$$

can be defined as a characteristic temperature and,

$$t_c = \frac{k \rho c}{(h_T)^2}$$

is defined as a characteristic time. To obtain the ignition delay time (t_{ig}) the surface temperature (T_s) is substituted by T_{ig} and equation (6) can be rewritten as:

$$T_{ig} = T_\infty + \bar{T} \left[1 - e^{t_{ig}/t_c} \operatorname{erfc} \left(\left(\frac{t_{ig}}{t_c} \right)^{1/2} \right) \right] \quad (7)$$

To solve for the ignition delay time (t_{ig}) a first order Taylor series expansion of equation (7) is conducted. The range of validity of this expansion is limited, thus can not be used over a large

range of incident heat fluxes. Consequently, the domain has to be divided at least in two. For this purpose a characteristic time to ignition,

$$\bar{t}_{ig} = \frac{k\rho c(T_{ig} - T_{\infty})^2}{[\dot{q}_s''(0,t)]^2}$$

can be defined by scaling the boundary condition of equation (5). The first domain corresponds to high incident heat fluxes where the ignition temperature (T_{ig}) is attained very fast, $\bar{t}_{ig} \ll t_c$.

Application of the first order Taylor Series Expansion to equation (7) around $t_{ig}/t_c \rightarrow 0$ yields the following formulation for the ignition delay time (t_{ig}):

$$\frac{1}{\sqrt{t_{ig}}} = \frac{2}{\sqrt{\pi}} \frac{a}{\sqrt{k\rho c}} \frac{\dot{q}_i''}{(T_{ig} - T_{\infty})} \quad (8)$$

As can be seen from equation (8), the short time solution for the ignition delay time (t_{ig}) is independent of the total heat transfer coefficient term (h_T). For low incident heat fluxes $\bar{t}_{ig} \gg t_c$ the Taylor series expansion around $t_{ig}/t_c \rightarrow \infty$ yields:

$$\frac{1}{\sqrt{t_{ig}}} = \frac{\sqrt{\pi} h_T}{\sqrt{k\rho c}} \left[1 - \frac{h_T(T_{ig} - T_{\infty})}{a\dot{q}_i''} \right] \quad (9)$$

The use of the appropriate simplified solution will allow the evaluation of the ignition delay time (t_{ig}) over the entire domain of imposed incident heat fluxes. By making $t_{ig} \rightarrow \infty$ in equation (9) a minimum external heat flux that will lead to ignition (at thermal equilibrium) can be extracted:

$$\dot{q}_{0,ig}'' = \frac{h_T(T_{ig} - T_{\infty})}{a} \quad (10)$$

It is important to note that determination of the fuel material properties (a , k , ρ , c) by experimentally obtaining t_{ig} in the domain where $t_{ig}/t_c \rightarrow 0$ (high heat fluxes) will lead to

values that are independent of the environmental conditions. In contrast, $\dot{q}_{0,ig}''$ is dependent on h_T , therefore is affected by nature of the convective flow parallel to the surface and the adequate determination of heat losses (h_T).

Values for the total heat transfer coefficient (h_T) have been shown to vary with orientation and environmental effects. Examples of typical values found in the literature are: $8.0 \text{ Wm}^2\text{K}^{-1}$ for natural turbulent convection and a vertical sample (Kashiwagi, 1982), $13.5 \text{ Wm}^2\text{K}^{-1}$ for a horizontal orientation (Atreya et al., 1985) and up to $15.0 \text{ W/m}^2\text{K}^{-1}$ obtained by Mikkola and Wichman (1989) while conducting experiments on a vertical orientation with wood. The total convective heat transfer coefficient (h_T) will be discussed in detail later.

Flame Spread (V_f)

In the presence of a flame and following similar assumptions as those presented above (Quintiere, 1981) a general expression can be obtained for the temperature at the fuel surface at any specific location

$$T_s = T_\infty + \bar{T} \left[1 - e^{t/t_c} \text{erfc} \left((t/t_c)^{1/2} \right) \right] + \frac{2}{\sqrt{\pi}} \frac{\dot{q}_f''}{h_T} \sqrt{\frac{\delta_f}{V_f t_c}} \quad (11)$$

Where V_f is the flame spread velocity, δ_f the characteristic length scale of the zone upstream preheated by the flame and \dot{q}_f'' the heat per flux provided by the flame.

The contribution of the external heat flux is represented by the surface temperature distribution upstream of the flame, $T_{s,i}(t)$, and corresponds to

$$T_{s,i}(t) = T_\infty + \bar{T} \left[1 - e^{t/t_c} \text{erfc} \left(\left(\frac{t}{t_c} \right)^{1/2} \right) \right] \quad (12)$$

For the flame to propagate T_s has to attain the ignition temperature, T_{ig} aided by the external heat flux and the heat flux provided by the flame. The flame, thus, has to bring the

surface temperature from $T_{S,i}(t)$ to T_{ig} for propagation to proceed and equation (11) can be re-written as follows

$$T_{ig} = T_{S,i}(t) + \frac{2}{\sqrt{\pi}} \frac{\dot{q}_f''}{h_T} \sqrt{\frac{\delta_f}{V_f t_c}} \quad (13)$$

It is a standard procedure for flame spread tests using the LIFT apparatus to preheat the sample until the surface attains thermal equilibrium before the flame is initiated. This leads to a definition of a characteristic time (t^*) beyond which no further changes in the fuel surface temperature occur and an initial surface temperature, $T_{S,i}^*$, can be defined as:

$$T_{S,i}^* = T_\infty + \bar{T}$$

This allows to define $T_{S,i}$ as a function of the external heat flux applied at each specified location of the sample.

In the particular case of crude oils thermal equilibrium can not be attained since, the fuel will be modified throughout the pre-heating process. Flame spread has to be studied under transient heating conditions. Furthermore, precursor flames (Glassman and Dryer, 1980, Ross, 1994) will further modify the pre-heating process upstream of the flame. Therefore temperature measurements immediately upstream of the flame will be used instead of using any analytical determination of $T_{S,i}(t)$. For simplicity, these experimental values will be denoted as $T_{S,i}$. Substituting $T_{S,i}$ in equation (13) and re-arranging

$$\frac{1}{\sqrt{V_f}} = \frac{\sqrt{k\rho c}}{a\sqrt{\phi}} (T_{ig} - T_{S,i}) \quad (14)$$

Where ϕ can be considered a constant that encompasses all the unknown parameters of the problem ($\delta_f, \dot{q}_f'', h_T$), is given by

$$\phi = \frac{4}{\pi} \left(\frac{\dot{q}_f'' h_T}{a} \right)^2 \delta_f \quad (15)$$

and represents the net thermal contribution of the flame to the spread process.

EXPERIMENTAL RESULTS

The experimental results will be presented in three different sections. First the results corresponding to the flash point temperature measurements will be discussed followed by the flame spread results and finally by the ignition tests. Results will be presented for two different crude oils, Alaska North Slope (ANS) and Cook Inlet (CI). Some preliminary results with SAE-30W oil will also be included. Experiments were conducted with fresh and weathered oils.

Closed Cup Flash Point

Flash point test results for the crude oils as a function of the mass loss due to weathering are presented in figure 8. Each point in the figure represents the average of 10 tests conducted in accordance with ASTM D56 standard. As seen from the figure, flash points extracted using the ASTM D56 closed cup tester have a linear dependence on the level of evaporation for both crude oils. More importantly, the flash points for ANS crude oils are significantly higher than the Cook Inlet crude. Note that data is only presented for flash points above ambient ($>20^\circ\text{C}$), since no ignition tests have been conducted for temperatures lower than ambient.

Since the pioneering work of Akita (1971), closed cup flash point temperatures have been shown to mark a transition between a uniform flame spread regime and a pre-mixed type spread. Numerous studies have shown similar results for pure and complex fuels (White et al., 1997). Both Glassman and Dryer (1980) and Ross (1994) warn on the uncertainties related to this parameter. Although, the theoretical flash point describes the liquid temperature at which the vapor pressure provides a lean-limit concentration at the pilot location (Ross, 1994), the

experimentally determined values are subject to buoyancy/stratification, pilot location, environmental conditions, etc. Furthermore, when using complex fuels such as crude oils, the equilibrium conditions might not necessarily be attained under realistic conditions. Closed cup flash point temperatures might under or over predict, depending on the fuel and environmental conditions, the fuel temperature that will lead to ignition.

Based on the above information, the flash point temperature, as obtained from ASTM D56 will be used as a starting point for a more detailed analysis of the ignition temperature (T_{ig}) to be used to interpret ignition and flame spread results.

Flame Spread

Flame spread over liquid fuels is a complex phenomenon that involves the understanding of natural convection inside the fuel layer as well as the chemical and thermal aspects leading to ignition in the gas phase. Studies as early as that of Mackinven et al. (1970) have identified a number of different experimental parameters that have a significant effect on the rate of flame spread. In specific, the purity of the fuel, the mode of ignition, the temperature of the fuel, the dimensions and material of the fuel container and the depth of the fuel layer affect the flame spread velocity. Reproducible experiments are, thus, very difficult to achieve specially with fuels as complex as crude oils and under conditions that will provide results that can be extrapolated to large scale fires. The mechanisms controlling the spread rate are still not fully understood and the state of the art is described in detail by Glassman and Dryer (1980) and more recently by Ross (1994).

The present work attempts to determine an experimental methodology that will allow simple determination of characteristic fuel properties that could help for the determination of protocols for in-situ burning of oil spills. The treatment that the flame spread process will be

given in this section might seem too simple for such a complex subject, but the objective of this work is to provide global criteria that will serve to describe the propensity of a fuel to sustain flame spread. Thus, average spread rates will be considered instead of tracking the pulsating flame front, and the controlling heat transfer mechanisms in the liquid phase will not be explored independently but lumped in the parameter ϕ .

Qualitative Observation and Physical Description of the Spreading Flame

After ignition, a fully developed flame is preceded by a pulsating blue flame very close to the surface. This form of propagation can be frequently found in the literature for sub-flash point propagation of a flame over a liquid fuel. The mechanisms leading to this form of propagation are well described by Glassman and Dryer (1981) and Ross (1994). Figure 9 shows three distinctive regions of the flame, the precursor flame, the transition flame and the fully developed flame (Mackinven et al., 1970). The precursor flame pulsates and the amplitude and frequency vary with the surface temperature. The precursor flame is blue and radiates weakly. In contrast, the leading edge of the transition zone is marked by a sudden transition to a bright yellow flame, propagates without pulsation and is easier to track. The boundary between the precursor flame and the transition zone is clearly delimited (Figure 9, (2)). The evolution towards the fully developed flame is smooth therefore no clear boundary between these two zones can be established (Figure 9 (3)). For this work, the movement of the tip of the stable yellow flame will be used to track the flame propagation front. Although the precursor flame is the real leading edge, its size, pulsating frequency and existence is governed by experimental conditions, therefore introduces uncertainty in the calculation of the spread rate.

The same three fuels, as for ignition tests, were used for flame spread tests (SAE-30W oil, ANS and Cook Inlet crude oils). SAE 30 weight oil is used for calibration because of its pure

characteristics and known properties. Concentration however, will be given to ANS and Cook Inlet crude oils at various levels of weathering, therefore no data will be presented for SAE 30 weight oil. All flame spread test are conducted using the unlined 1.2 mm thick stainless steel tray illustrated in figure 3. Fuel surface temperature measurements are obtained using thermocouples placed in the center axis of the flame spread tray with the tip as close to the surface as possible. Flame speed and surface temperature are recorded for each test. Various fuel layer thickness are obtained by adjusting the gross volume of supporting water and the corresponding amount of fuel.

Extreme care was taken to control initial conditions, which are needed for reproducible flame spread data. External air currents are standardized by adjusting the flow of the overhead hood. Temperatures of the water sublayer and fuel are carefully monitored prior to each test and maintained at the ambient room temperature of $22^{\circ}\text{C} \pm 0.5^{\circ}\text{C}$. Fuel and water are added to the flame spread tray and time is allowed for currents in the air and liquid to subside before exposure to external radiation.

For all tests, there is a 1mm free board height above the fuel surface to the rim of the flame spread tray. Under external heating, the liquids are not expected to immediately ignite and thus, require additional capacity for expansion during testing. Studies have shown (Mackinven et al.,1970) that the freeboard can result in a drop of approximately 20% on the flame spread velocity due to obstruction of the air flow, therefore care was taken to keep the freeboard height as small as possible.

Although ignition results will be presented in a later section, ignition tests were conducted prior to the flame spread tests and a minimum heat flux necessary for piloted ignition ($\dot{q}_{o,ig}''$) was obtained together with a minimum heat flux that will prevent boiling of the water

sub-layer ($\dot{q}_{o,B}''$). After determination of the critical heat fluxes for ignition ($\dot{q}_{o,ig}''$) and boiling ($\dot{q}_{o,B}''$), an external radiant flux is selected to avoid boiling of the water sub-layer prior to ignition. The sample is, therefore, heated at $\dot{q}_{o,ig}'' + 5 \text{ kW/m}^2$ until piloted ignition occurs at the end nearest to the radiant panel. Flame spread measurements are recorded using a high resolution 8mm video camera operating at 30 frames per second. After the flame has spread to the end of the tray and the necessary measurements have been taken, the flame is extinguished by covering the tray with a smother board.

Numerous techniques are available for measuring the rate of progress of the flame across the surface of the fuel. Some simple methods give a mean velocity of spread while other more complex, time-consuming methods produce instantaneous spreading velocities at a particular position. In this work, three techniques are employed to measure flame spread: stopwatch timing between two fixed points, cinematography of flame position and time and surface thermocouple measurements. The thermocouples also provide the fuel surface temperature at the instant prior to flame propagation at each reference point. In most flame spread tests, a combination of all three of the above techniques is utilized. Redundancy allows for visual calculation to be backed by numerical confirmation of the propagation front.

A representative surface temperature evolution is presented in Figure 10. This particular case corresponds to a 20% weathered ANS crude oil 8 mm bed and is representative of all other conditions studied. Initially, the surface is preheated by the radiation from the external source. Consequently, thermocouples positioned nearest to the radiant panel reflect a higher temperature. The distance given with each thermocouple history corresponds to the distance from the trailing edge of the tray. When the temperature of the fuel surface approaches the ignition temperature (in the area of highest heat flux) and in the presence of the pilot flame, the gaseous mixture

ignites. The sudden peak in recorded temperatures indicates this event. The flame, then, propagates down the sample. The thermocouple traces show a sudden increase followed by a change in slope, which generally leads to a second sudden increase. The thermocouples seem unaffected by the precursor flames and the first sudden increase corresponds to the leading edge of the transition flame. The change in slope and second peak generally corresponds to the emergence of the thermocouple tip once the fully developed flame has reached the thermocouple. Thermocouples are some times not sensitive to these changes in slope (i.e. thermocouple labeled 350 mm), this is mainly due to inadequate positioning of the thermocouple. Thermocouple misplacement is very difficult to correct therefore will be accepted as a source of error.

Figure 10 shows uneven preheating before the temperature jump that represents the flame reaching the thermocouple. As can also be observed the temperature histories have not reached steady state conditions. The surface temperature used to correlate the data is that recorded immediately before the first peak. Determination of the actual surface temperature at the arrival of the flame is quite complicated under these circumstances and significant scatter of the data is expected but should not preclude the determination of the global parameters that describe the spread process.

Experimental Results

The $V_f^{-1/2}$ is plotted as a function of $T_{S,i}$ according to equation (14) and presented in Figure 11 for ANS and Figure 12 for Cook Inlet crude oils. Although the data shows the expected scattering it follows the linear trends predicted by equation (14).

Figure 11 shows a significant effect of weathering on the flame spread velocity. Highly weathered fuels propagate much slower (i.e. 20% mass loss) than lightly weathered oils (8% mass loss). Fresh ANS was not used for flame spread since ignition was almost instantaneous.

It is important to note that although the propagation velocities are very different, the slope of the line fit to the experimental data seems constant.

Data was collected for 8 mm (empty symbols) and 3 mm fuel layers (filled symbols). For lightly weathered fuels, where propagation is fast, the fuel layer thickness seems to have no effect on the propagation velocity. As the propagation velocity decreases (12% mass loss) a difference between the different thickness layers appears, becoming marked for 20% mass loss. For this case flame spread over an 8 mm layer is significantly faster than for a 3 mm layer.

Similar tests conducted for Cook Inlet crude oil (Figure 12) show comparable results. Data is presented for layers 3 mm and 8 mm thick and for three weathering levels, 25%, 20% and 13%. Tests were not conducted for lower mass losses because spread rates were almost instantaneous and the effect of the external heat-flux could not be quantified. The data shows similar trends to those presented for ANS. The propagation velocities are comparable and follow linear trends. Scattering is again significant. The marked difference between Cook Inlet and ANS crude oils is that for the former the fuel layer thickness seems to have no effect on the flame spread rate.

It is important to note that the external heat flux was chosen to preclude boiling of the waterbed before arrival of the fully developed flame. Flame spread is fast enough that subsequent water boiling at the trailing edge will not affect the spread velocity of the leading edge of the flame. The necessary heat flux that will preclude boiling was established by Wu et al. (1998).

The data as presented in Figures 11 and 12 is difficult to compare since the lack of a fuel ignition temperature precludes the proper correlation with equation (14). Despite the reservations on the use of the flash point as a fuel ignition temperature (T_{fi}), this value will be

used to attempt correlation of the data. The results of this correlation are presented in Figures 13 (for ANS crude oil) and 14 (for Cook Inlet crude oil). The values presented are average values for each heat flux and the error bars show the maximum discrepancies from the average.

By presenting the data in this fashion an “ignition temperature” can be extracted by linear extrapolation of the data through the temperature axis. Although not a real ignition temperature, T_{ig} is representative of the energy balance necessary at the surface to allow gas phase propagation of a flame. This corresponds to the critical condition ($\dot{q}''_{0,ig}$) for both ignition and flame spread tests (equation 10) therefore, can be used in the correlation of the ignition data.

In the case of ANS crude oil, weathering results in a decrease on the ignition temperature relative to the flash point temperature (Figure 13). For 8% mass loss the ignition temperature is approximately 30 °C greater than the flash point temperature, 20°C for 12% converging towards the flash point temperature for 20%. Complex fuel mixtures such as crude oils are formed by different hydrocarbons. As the more volatile fractions evaporate leading to ignition, the heavier hydrocarbons continue to heat up resulting in ignition temperatures higher than the flash point temperature. At higher weathering levels, the flash point temperature of the individual fractions left become comparable.

A decrease in fuel layer thickness can also result in an increase in the relative difference between the flash point temperature and the ignition temperature. For a fully developed flame to propagate a minimum net heat flux at the surface is necessary. As described first by Roberts and Quince (1973) and then summarized by Ross (1994), a critical mass transfer number (“B”) can be defined for different fuels. A decrease in the fuel layer thickness will lead to increased heat losses from the fuel to the waterbed underneath. The analytical approach assumes a semi-infinite bed, therefore, the increase in heat losses will be translated into a decreased “B” and

consequently on an increased T_{ig} or necessary contribution of the external heat flux to sustain propagation.

An alternate approach will be to obtain a solution that incorporates both layers and their different thermal diffusivities. The solution will require a numerical approach which will defeat the practical nature of this study.

Cook Inlet crude oil behaves slightly different. Even when weathered as much as 25% mass loss, Cook Inlet crude oils still has a flash point temperature lower than 60°C showing the large presence of light fractions. Flame spread is consequently fast and requires low surface temperatures. Under these conditions, the influence of the water bed and of the weathering level can not be noticed when correlating the spread data as a function of $(T_{fl}-T_{s,i})$ as shown in Figure 14.

For both crude oils the slope of the data remains almost independent of the experimental conditions. For ANS and specially for Cook Inlet crude oil, the data seems to converge towards a fixed ignition temperature ($\approx T_{fl} + 30^{\circ}\text{C}$) which might correspond to the temperature at which flame propagation can be fully considered a gas phase phenomena. This is an important observation because it shows that, when assisted by external radiation or in a real scenario, by radiative feedback from the plume, propagation can occur by burning of the lighter fractions with the heavier hydrocarbons being unaffected. Once the flame has propagated through the surface, burning of the heavier fractions will follow.

Ignition Delay Time

A series of tests were conducted with two crude oils. Figure 15 shows the results ANS crude oil and Figure 16 for Cook Inlet crude oil. Figure 15 also includes data by Putorti et al. (1994). The data presented is an average of at least five experiments conducted under identical

conditions. Only selected error bars are presented to avoid crowding of the figures, these were selected to show the maximum discrepancies of individual experiments from the average.

After pouring the liquid fuel on the water subsurface, time is allowed for gaseous and liquid currents to subside. A radiation shield (calcium silicate board) is placed in front of the panel before the sample is introduced to its test position (Figures 1 and 2). Once the sample has been placed, the radiation shield is removed and time recording starts. The ignition delay time is established as the time required for the flame to fully establish for better correlation with the flame spread results.

It was observed that ANS crude oil in its natural state ignited at ambient temperature, therefore no external heat flux was necessary for ignition. The ignition delay time decreases as the heat flux increases, and a linear dependency between the external heat flux and $t_{ig}^{-1/2}$ is obtained. Non-ignition data is presented on the “ \dot{q}_i'' ” axis since the time for ignition was assumed to approach infinity. As can be seen in Figure 15, extrapolation of the linear regression to determine $\dot{q}_{0,ig}''$ from the intercept provides a fairly good approximation. The intercept with the horizontal axis does not necessarily provide the critical heat flux for ignition since, for low external heat fluxes, equation (8) does not approximate anymore equation (7), instead equation (9) better represents t_{ig} . Studies have shown that this approximation can introduce significant errors in the evaluation of $\dot{q}_{0,ig}''$ for different solid fuels (Mikkola and Wichman, 1989, Quintiere, 1981, Quintiere et. al, 1983 and Quintiere and Harkleroad, 1984) but this is not the case for the crude oils studied in the present work. The linear extrapolation was preferred since the critical $\dot{q}_{0,ig}''$ is very low for some of the fuels and, therefore, difficult to obtain experimentally using the HIFT radiant panel.

The linear extrapolation resulted in negative values of $\dot{q}_{0,ig}''$ for the fresh and slightly weathered fuels. Negative values imply that the fuel will ignite at ambient temperature. Figures 15 and 16 show that the critical heat flux for ignition will increase with weathering. The critical heat flux corresponding to the data reported by Putorti et al. (1994) fits well with the data collected in the present work. The slope obtained from the data of Putorti et al. (1994) is different than the one obtained through this work, this discrepancy was studied by Wu et al. (1998) who showed that in the absence of a forced flow t_m is large and can not be neglected and a significant difference on the ignition delay time results. In contrast, at low heat fluxes, t_v is large, therefore the variations, due to t_m , are less obvious and there is coincidence in the values of $\dot{q}_{0,ig}''$ obtained.

Preliminary experiments with SAE30W oil showed that as the heat flux decreases boiling of the water bed occurred, boiling perturbed the fuel layer precluding ignition. A minimum heat flux, $\dot{q}_{0,B}''$, was found to be necessary for ignition and to avoid boiling of the water. The magnitude of $\dot{q}_{0,B}''$ has a linear dependency with the fuel layer thickness and can be predicted by using the fuel layer thickness as the characteristic penetration depth, $\delta_F = \sqrt{\alpha t_{ig}}$, and substituting equation (8) for t_{ig} . A detailed study on this particular aspect of the problem work and can be found in Wu et al. (1998).

For the present tests, the fuel layer thickness was chosen ($\delta_F > 5$ mm) to guarantee proper determination of $\dot{q}_{0,ig}''$. As mentioned before, if the fuel layer is too thin, boiling is attained and truncates the ignition delay time curves. A few selected results, for $\delta_F < 5$ mm, are presented in figure 16 and show that away from $\dot{q}_{0,ig}''$ the effect of the water bed on t_{ig} is present but not dramatic. The results presented in Figure 16 are for Cook Inlet oil, this fuel is chosen because

ignition occurs before boiling of the waterbed (for a 3 mm fuel layer), thus the effect of the water bed can be observed independent of water boiling.

The dotted lines show the trends followed by a 3 mm fuel layer, it can be seen that the slope changes slightly leading to higher values for $\dot{q}_{0,ig}''$. The water acts as a heat sink decreasing the value of the global thermal inertia, thus increasing the slope of the line fits or the value of $a/\sqrt{k\rho c}$. In contrast, equation (10) and the constant T_{ig} value found in the previous section shows that the water should have no effect on the $\dot{q}_{0,ig}''$. Equation (10) is derived by introducing $t_{ig} \rightarrow \infty$ in equation (7), therefore assumes that the fuel and water have attained the thermal equilibrium temperature, therefore there is no in-depth heat flux. This is clearly not the case for the present study where ignition occurs fast and in-depth heat flux is still present, thus is affected by the waterbed. This discrepancy provides an estimate of the error incurred when fitting equation (8) as far as $\dot{q}_{0,ig}''$ ($\sim 1 \text{ kW/m}^2$). Discrimination of this order of magnitude could not be obtained from the radiant panel so will be accepted as the magnitude of the error for $\dot{q}_{0,ig}''$.

The critical heat flux for ignition ($\dot{q}_{0,ig}''$) as obtained from figures 15 and 16, is presented in figure 17. Results are presented for Cook Inlet and ANS crude oils for different fuel layer thickness. The increasing value of $\dot{q}_{0,ig}''$ with mass loss shows that the weathering makes ignition more difficult. Figure 17 shows clearly the discrepancy between the critical heat flux for ignition for 3 mm as opposed to almost identical values obtained for 8 and 15 mm layers. As mentioned before, for ANS crude oil T_{ig} increases as the fuel layer thickness decreases to 3 mm leading to a higher critical heat flux for ignition providing justification for the differences presented in Figure 17. No specific reason for this discrepancy can be concluded, but it can be noted that this discrepancy includes the error introduced by the determination of the $\dot{q}_{0,ig}''$ and the increasing

effect of boiling before attaining $\dot{q}_{o,ig}''$. The conclusion extracted from this data will be therefore based only on the 8 mm and 15 mm layers.

Based on values of $\dot{q}_{o,ig}''$, ANS crude oil was observed to be more prompt to ignition than Cook Inlet crude oil. Cook Inlet ignited without an external heat flux for a mass loss rate smaller than 10%, and ANS crude oil for a mass loss smaller than 7%. The results presented are representative of all other cases studied.

A comparison of the ignition temperature and the critical heat flux for ignition obtained from the ignition tests is presented in figure 18. The data points correspond to different levels of weathering. It is noticed that the ignition temperature has a linear dependence with the critical heat flux for ignition, as predicted by equation (10). The line fit covers both ANS and Cook Inlet crude oils and converges to a temperature of 52°C for $\dot{q}_{o,ig}''=0$. By using equation (10), the global thermal efficiency (a/h_T) can be evaluated since a/h_T corresponds to the inverse of the slope of the line fit. As shown by equation (2), the global heat transfer coefficient consists of both a radiative and convective component. Since the convective component is a function of the orientation and flow conditions and independent of the fuel, the slope of the data presented in figure 18 provides an indirect measure of the linearized radiative heat transfer coefficient showing no difference between both fuels.

Finally, $\sqrt{k\rho C}/a$ was calculated using equation (8) and substituting the values for T_{ig} determined from the flame spread data. The value of $\sqrt{k\rho C}/a$ is obtained for all ignition tests and presented as a function of the external heat flux. Figure 19 presents the values for ANS and figure 20 for Cook Inlet. The correlation of the data is good although some scattering can be observed. For ANS the scattering of the data shows no clear trend with respect to any of the

parameters varied, instead for Cook Inlet the data corresponded to the least weathered oil (8%) shows a higher value of $\sqrt{k\rho C} / a$ than those corresponding to more weathered fuels. As shown by the spread data, evaporation occurs during the pre-heating period, and since equation (8) assumes inert heating of the fuel, the latent heat of evaporation might contribute to the artificially increased value for $\sqrt{k\rho C} / a$.

Summary and Conclusions

A methodology to provide a comprehensive evaluation of the flammability of liquid fuels by experimentally determining the flame spread rate and the ignition delay time as a function of an externally imposed radiative heat flux has been developed and used to evaluate the effect of weathering and fuel layer thickness on the flammability of crude oils. Determination of the closed cup flash point temperature has been used to complement this methodology. The specific application is that of in-situ burning of oil spills.

The flame spread velocity was presented in a form that corresponds to equation (14). A preliminary correlation by means of the flash point temperature allowed to determine the effect of the fuel layer thickness and weathering. These effects can be translated into an ignition temperature. The ignition temperature converges to the flash point temperature for highly weathered fuels and to a temperature that will lead to gas phase propagation for lightly weathered fuels. The ignition temperature will also converge to the same value for thin fuel layers where the water bed represents a significant heat sink. The ignition temperature is obtained from the intercepts of the spread data with the temperature axis. Cook Inlet sustained gas phase propagation for all conditions studied while ANS progressed towards condensed phase flame spread as the weathering level increased.

The ignition data was presented in a form that corresponds to equation (8) and provides estimates of the evolution of $\sqrt{k\rho c}/a$ (thermal inertia of the fuel). By using the ignition temperature obtained from the flame spread data, a value of $\sqrt{k\rho c}/a \approx 2,800 \text{Ws}^{1/2} / \text{m}^2\text{K}$ for ANS crude oil and $\sqrt{k\rho c}/a \approx 2,100 \text{Ws}^{1/2} / \text{m}^2\text{K}$ for Cook Inlet. Both values remained invariant with the weathering level. In contrast, the critical heat flux for ignition increased with the mass loss due to weathering with Cook Inlet crude oil showing consistently lower values. The critical heat flux for ignition together with the ignition temperature serve to determine the parameter (a/h_T) , which is an estimate of the efficiency of the heat transfer process at the fuel gas phase interface. Both fuels showed a consistent value of $a/h_T \approx 0.008 \text{m}^2\text{K/W}$. This parameter is a combination of the environmental conditions and the radiative properties of the fuel, therefore its quantitative value depends on the experimental conditions and should not be extrapolated to other scenarios. Nevertheless, if the flow conditions are kept invariant, this parameter will provide a means to compare the efficiency of the heat transfer process at the fuel/air interface.

Finally, the contribution of the flame heat flux can be extracted through the parameter ϕ (equation (14)). For both fuels an approximate value of $1.5 \times 10^8 \text{W}^2\text{s}^2/\text{m}^4$ was obtained. By substituting a/h_T , on equation (15), all non-flame related parameters can be eliminated from ϕ , this could be done in an attempt to eliminate the environmental dependency of ϕ but will not be done here. It has been shown (Chen and T'ien, 1986) that the characteristic pre-heat length upstream of the flame is strongly dependent on the flow characteristics ($\delta_i = \alpha/U$), thus, can not be considered independent of the environment. For these reasons, ϕ will be kept as shown in equation (15) and will be considered a parameter that provides a relative evaluation of the contribution of the flame to the spread process, thus, can be used for comparison between different fuels, but not extrapolated to different scenarios.

Acknowledgements

This work was funded by NIST and the M. S. Wirt Foundation. The insightful comments of Prof. M. diMarzo have greatly contributed to this work. The flash point temperature measurements were conducted by S. Olenick and T. Mosman.

References

Akita, K. and Fujiwara, O., "Pulsating Flame Spread along the Surface of Liquid Fuels," *Combustion and Flame*, 17, 268-269, 1971.

ASTM, ASTM Fire Test Standards, 3rd Edition, 1990.

ASTM, Annual Book of ASTM Standards, 1994.

Arai, M., Saito, K., and Altenkirch, R.A., "A Study of Boilover in Liquid Pool Fires Supported on Water, part I: Effect of a Water Sublayer on Pool Fires," *Combustion Science and Technology*, 71, pp25-40 1990.

Atreya, A., Carpenter, C., and Harkleroad, M., "The Effect of Sample Orientation on Piloted Ignition and Flame Spread," *Fire Safety Science – 1st International Symposium*, p.97-109, 1985.

Bobra, M., "A Study of the Evaporation of Petroleum Oils," Publication EE-135, Environmental Canada, Ottawa, Ontario, K1A OH3, 1992.

Brzustowski, T.A., and Twardus, E.M., "A Study of the Burning of a Slick of Crude Oil on Water," *Nineteenth Symposium (International) on Combustion*, The Combustion Institute, Pittsburgh, PA, pp847-854, 1982.

Carslaw, H.S. and Jaeger, J.C., *Conduction of Heat in Solids*, 2nd Edition, Oxford University Press, Oxford, pp70-76, 1963.

Chen, C.H. and T'ien, J.S. "Diffusion Flame Stabilization at the Leading Edge of a Fuel Plate," *Combustion Science and Technology*, **50**, 238-306, 1986.

Fernandez-Pello, A.C., "Combustion Fundamentals on Fire: The Solid Phase," *Academic Press*, pp31-100, 1995.

Fingas, M., "The Evaporation of Oil Spills: Variation with Temperature and Correlation with Distillation Data, *Proceedings of the 19th AMOP Technical Seminar*, Alberta, Canada, pp29-135, 1996.

Garo, J.P., Vantelon, J.P., and Fernandez-Pello, A.C., "Boilover Burning of Oil Spilled on Water," *Twenty-fifth Symposium (International) on Combustion*, The Combustion Institute, Pittsburgh, PA, pp1481-1488, 1994.

Garo, J.P. Vantelon, J.P. Gandhi, S. and Torero, J.L. "Some Observations on the Pre-Boilover Burning of a Slick of Oil on Water" *19th Arctic and Marine Oilspill Program (AMOP) Technical Seminar*, Calgary, Canada, vol.2, 1611-1626, June 1996.

Garo, J.P., Vantelon, J.P., Gandhi, S. and Torero, J.L. "Determination of the Thermal Efficiency Pre-boilover Burning of a Slick of oil on Water," *Spill Science and Technology Bulletin*, **5**, 2, 141-151, 1999.

Glassman, I., and Dryer, F., "Flame Spread Across Liquid Fuels," *Fire Safety Journal*, 3, pp123-138, 1980.

Hillstrom, W., "Temperature Effects of Flame Spreading Over Liquid Fuels", *Eastern States Section: Combustion Institute Fall Technical Meeting*, The Combustion Institute, 1975.

Inamura, T., Saito, K., and Tagavi, K.A., "A Study of Liquid Pool Fires Supported on Water. Part II: The Effect of In-depth Radiation Absorption," *Combustion Science and Technology*, Vol. 86, pp105-119, 1992.

Kanury, M. "Ignition of Liquid Fuels," *SFPE Handbook*, 2nd Edition, Society of Fire Protection Engineers, Quincy, MA, pp2.160-2.170, 1994.

Kashiwagi, T., "Effects of sample Orientation on Radiative Ignition," *Combustion and Flame*, 44, 223-245, 1982.

Kasiwagi, T., Mell, W.E., McGrattan, K.B. and Baum, H.R., "Ignition, Transition, Flame Spread in Multi-dimensional Configurations in Micro-Gravity," *Fourth International Micro-gravity Combustion Workshop*, NASA Lewis Research Center, pp411-416, 1997.

Kennedy, D., Barnea N., and Shigenaka, G., "Environmental and Human Health Concerns Related to In situ Burning", *Proceedings of the In Situ Burning Oil Spill Conference*, Orlando, Florida, pp47-56, 1994.

Koseki, H., Kokkala, M., and Mulholland, G.W., "Experimental Study of Boilover in Crude Oil Fires," *Fire Safety Science-Proceedings of the Third International Symposium*, pp865-875, 1991.

Mackinven, R., Hansel, J.G., and Glassman, I., "Influence of Laboratory Parameters on Flame Spread Across Liquid Fuels," *Combustion Science and Technology*, 1, pp293-306, 1970.

McAuliffe, C.D., "The Weathering of Volatile Hydrocarbons from Crude Oil Slicks on Water," *Proceedings Form the 1989 Oil Spill Conference*, San Antonio, Texas, pp357-363, 1989.

Mikkola, E., and Wichman, I.S., "On the Thermal Ignition of Combustible Materials," *Fire and Materials*, 14, 87-96, 1989.

Motevalli, V., Chen, Y., Gallagher, G., Sheppard, D., "Measurements of Horizontal Flame Spread on Charring and Non-Charring Material Using the LIFT Apparatus," *Fire and Materials*, Interscience Communications Unlimited, pp23-32, 1992.

Mudan, K.S. and Croce, P.A., "Fire hazard Calculations for Large Open Hydrocarbon Fires," *SFPE Handbook*, 2nd Edition, Society of Fire Protection Engineers, Quincy, MA, pp3-197-3-240, 1994.

Ostazeski, S.A., Daling, P.S., Macomber, S.C., Fredricksson, D.W., Durell, G.S., Uhler, A.D., Jones, M., and Bitting, K., "Weathering Properties and the Prediction Behavior at Sea of a Lapio Oil (weathered No. 6 Fuel Oil)", *Proceedings of the 19th AMOP Technical Seminar*, Alberta, Canada, 1996, pp137-162.

Petrov, A.A., Petroleum Hydrocarbons, Springer-Verlag, 1987.

Putorti, A., Evans, D., and Tennyson, E., "Ignition of Weathered and Emulsified Oils," *Proceedings from the Seventeenth Arctic and Marine Oil Spill Program Technical Seminar*, pp657-667, 1994.

Quintiere, J., "A Simplified Theory for Generalizing Results from a Radiant Panel Rate of Flame Spread Apparatus," *Fire and Materials*, 5, 2, pp52-60, 1981.

Quintiere, J., Harkleroad, M., and Walton, D., "Measurement of Material Flame Spread Properties," *Combustion Science and Technology*, 32, pp67-89, 1983.

Quintiere, J., and Harkroad, M., "New Concepts for Measuring Flame Spread Properties," U.S. Department of Commerce, NBSIR 84-2943, 1984.

Reijnjart, R. and Rose, R., "Evaporation of Crude Oil at Sea", *Water Research*, 16, pp1319-1325, 1982.

Roberts, A.F. and Quince, B.W., "A Limiting Condition for Burning of Flammable Liquids," *Combustion and Flame*, 20, pp245-251, 1973.

Ross, H., Ignition and Flame Spread Over Laboratory-Scale Pools of Pure Liquid Fuels," *Progress in Energy and Combustion Science*, 20, pp17-63, 1994.

Rusin, J., Lunel, T., and Davies, L., "Validation of the EUROSPILL Chemical Spill Model", *Proceedings of the 19th AMOP Technical Seminar*, Alberta, Canada, pp.1437-1485, 1996.

Sellers, C., Fox, B., Pautz, J., "Bartlesville Project Office Crude Oil Analysis Data Base User's Guide", Department of Energy, DOE/BC-96/3/SP, p4, March 1996.

Sirignano, W. and Glassman, I., "Flame Spreading Above Liquid Fuels: Surface-Tension-Driven Flows," *Combustion Science and Technology*, 1, pp307-312, 1970.

Tebau, P., "Operational Implications of In Situ Burning", *Proceedings of the In Situ Burning Oil Spill Conference*, Orlando, Florida, pp57-62, 1994.

Twardus, E.M. and Brzustowski, T.A., "The Burning of Crude Oil Spilled on Water," *Archivum Combustionis*, Polish Academy of Sciences, 1, 1-2, pp49-60, 1981.

Walavalkar, A.Y, Kulkarni, A.K., "A Comprehensive Review of Oil Spill Combustion Studies", *Proceedings from the 19th AMOP Technical Seminar, Calgary, Alberta, Canada*, pp1081-1104, July 1996.

White, D., Beyler, C.L., Fulper, C. and Leonard, J., "Flame Spread on Aviation Fuels," *Fire Safety Journal*, 28, pp1-31, 1997.

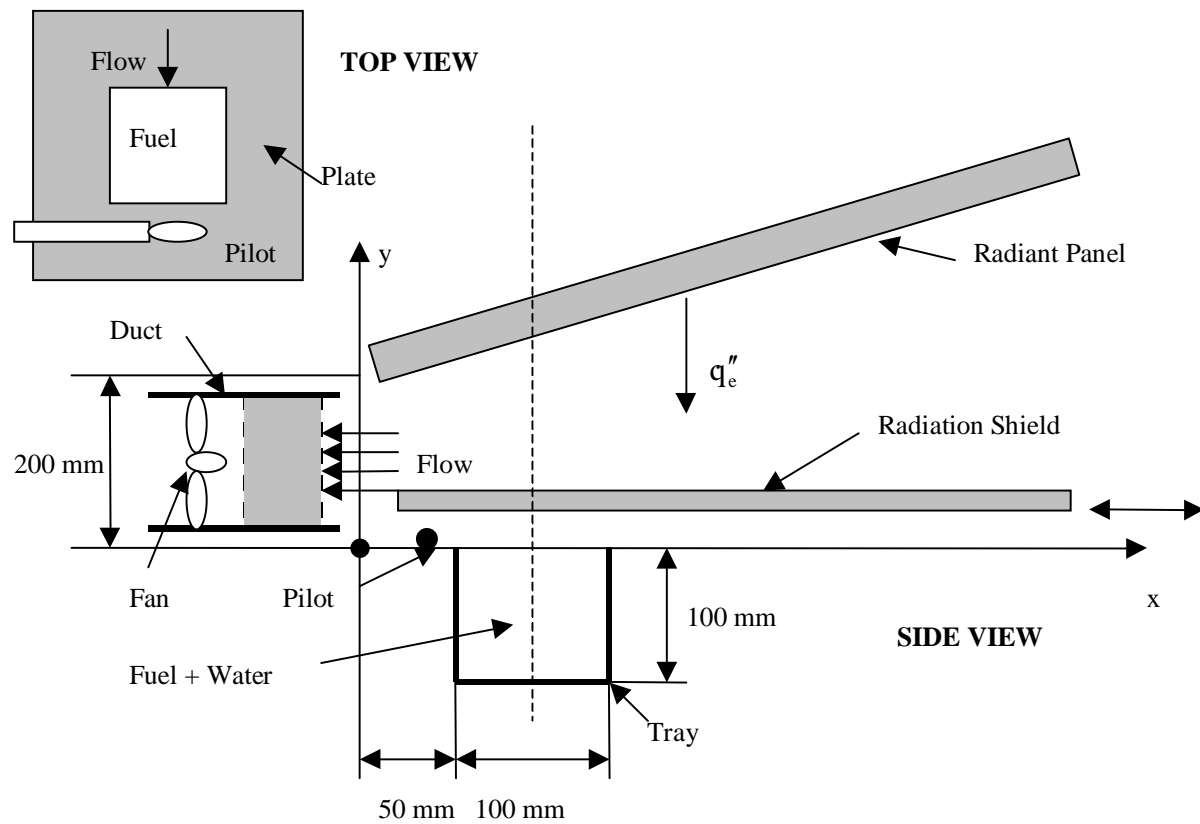
Wu, N., Baker, M., Kolb, G. and Torero, J.L. "Ignition, Flame Spread and Mass Burning Characteristics of Liquid Fuels on a Water Bed," *Spill Science and Technology Bulletin*, 3, N^o. 4, pp209-213, 1996.

Wu, N., Kolb, G. and Torero, J.L. "Piloted Ignition of a Slick of Oil on a Water Sublayer: The Effect of Weathering," *27th International Symposium on Combustion/The Combustion Institute*, pp2783-2790, 1998.

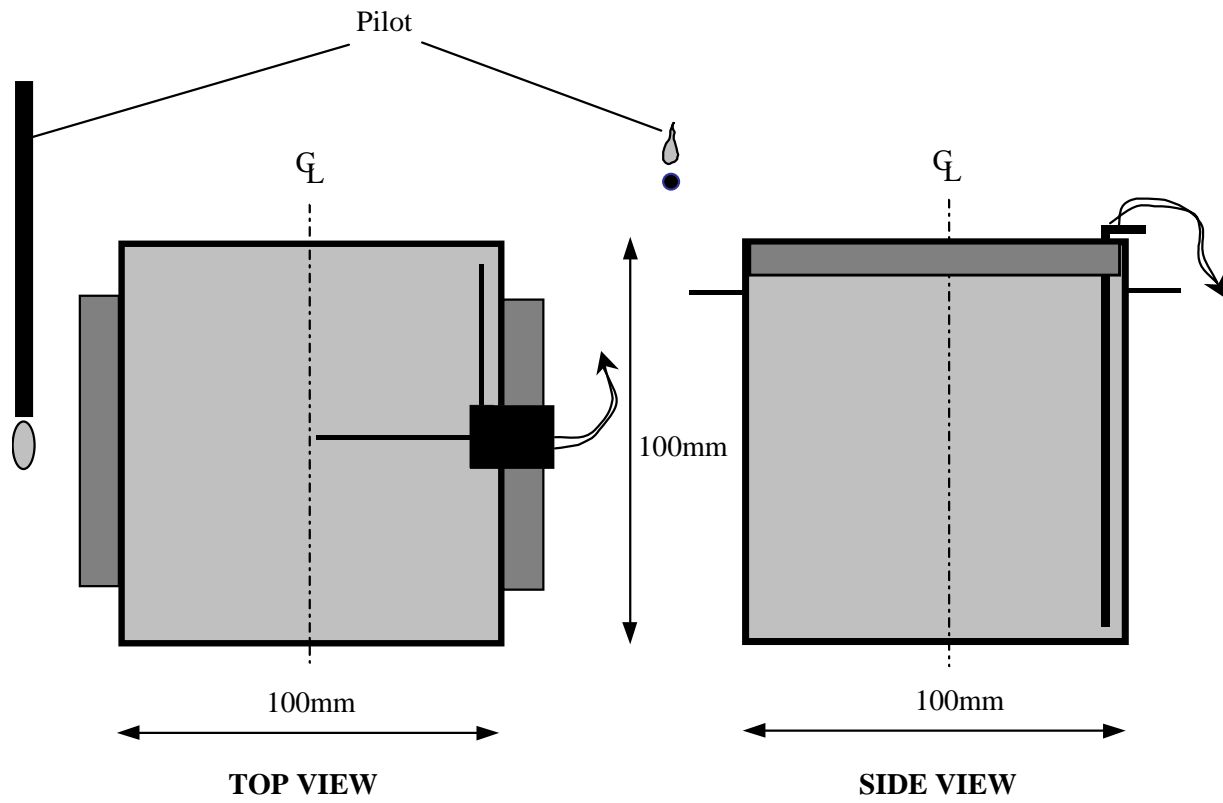
Wu, N. "*Piloted Ignition and Flame Spread of a Liquid Fuel on a Water Sub-Layer*" Masters Thesis, University of Maryland, College Park, 1998.

LIST OF FIGURES

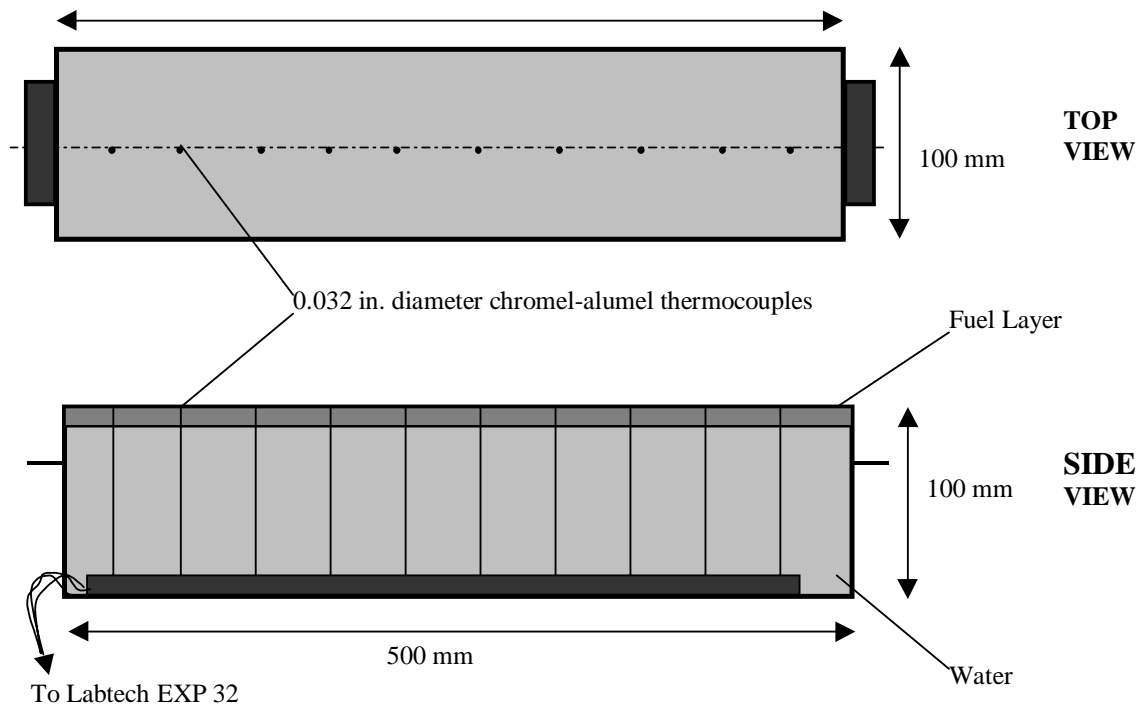
- Figure 1 - Schematic of the modified LIFT apparatus in the horizontal configuration.
- Figure 2 - Schematic of experimental ignition tray.
- Figure 3 - Schematic of experimental flame spread tray.
- Figure 4 - Plot of incident heat flux distribution of the experimental apparatus.
- Figure 5 - Cook inlet crude evaporation as function of the initial volume for specific times.
- Figure 6 - Cook inlet crude evaporation as a function of time for various rotator velocities.
- Figure 7 - Cook Inlet crude evaporation as a function of temperature for various times.
- Figure 8 - Flash points of ANS and Cook Inlet crude oils at various levels of weathering.
- Figure 9 – Schematic of the flame showing the precursor flame followed by a transition zone that develops to a fully developed flame.
- Figure 10 - Surface thermocouple temperatures for flame a spread test of 12% evaporated ANS crude (8mm fuel layer thickness).
- Figure 11 – Flame Spread Velocity as a function of the surface temperature prior to the arrival of the transition flame for ANS crude oil.
- Figure 12 – Flame Spread Velocity as a function of the surface temperature prior to the arrival of the transition flame for Cook Inlet crude oil.
- Figure 13 – Flame Spread Velocity as a function of the difference between the surface and the flash point temperature, prior to the arrival of the transition flame for ANS crude oil.
- Figure 14 – Flame Spread Velocity as a function of the difference between the surface and the flash point temperature, prior to the arrival of the transition flame for Cook Inlet crude oil.
- Figure 15 - ANS crude oil ignition delay time for various levels of evaporation.
- Figure 16 - Cook Inlet ignition delay time for various levels of evaporation.
- Figure 17 - $\dot{q}_{o,ig}''$ for ANS and Cook Inlet crude oils at various fuel layer thickness.
- Figure 18 - ASTM D56 closed cup flash point tests for ANS and Cook Inlet crude oils as a function of $\dot{q}_{o,ig}''$.
- Figure 19 - $\sqrt{k\rho C}/a$ as a function of the external heat flux for ANS crude oil.
- Figure 20 - $\sqrt{k\rho C}/a$ as a function of the external heat flux for Cook Inlet crude oil.



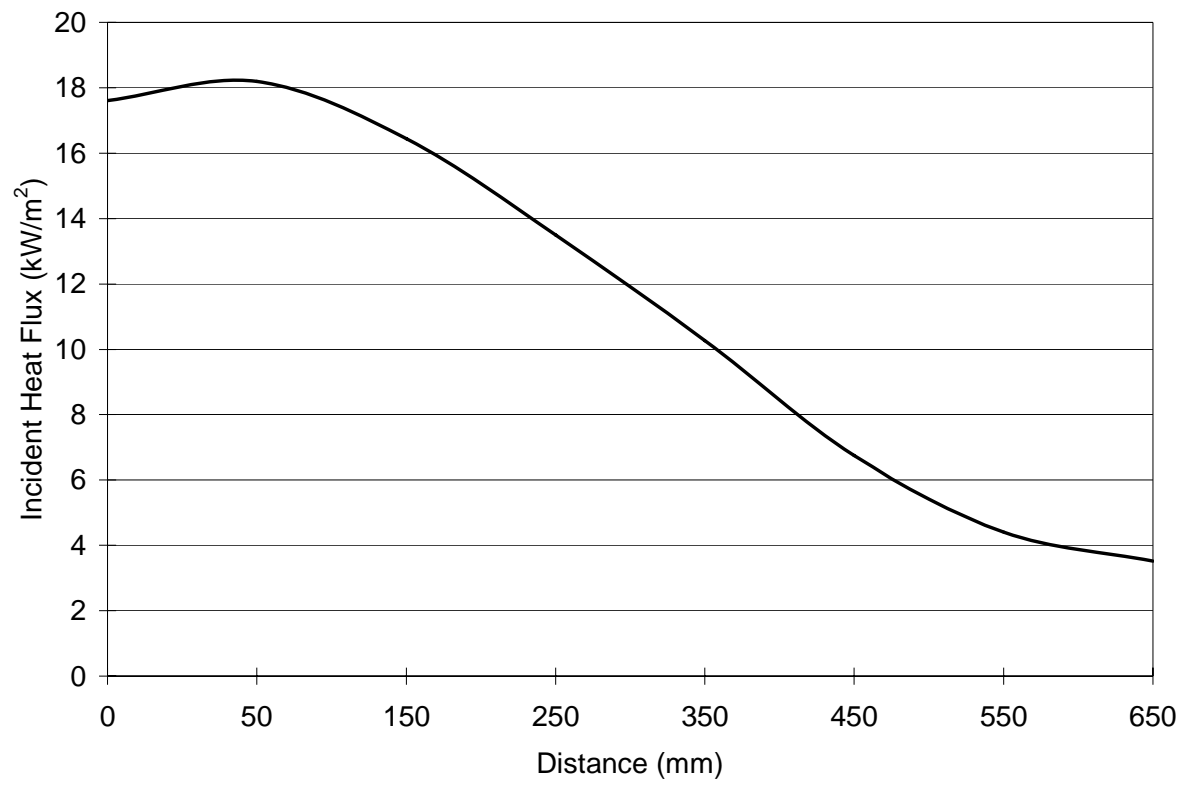
Wu et al.
Figure 1



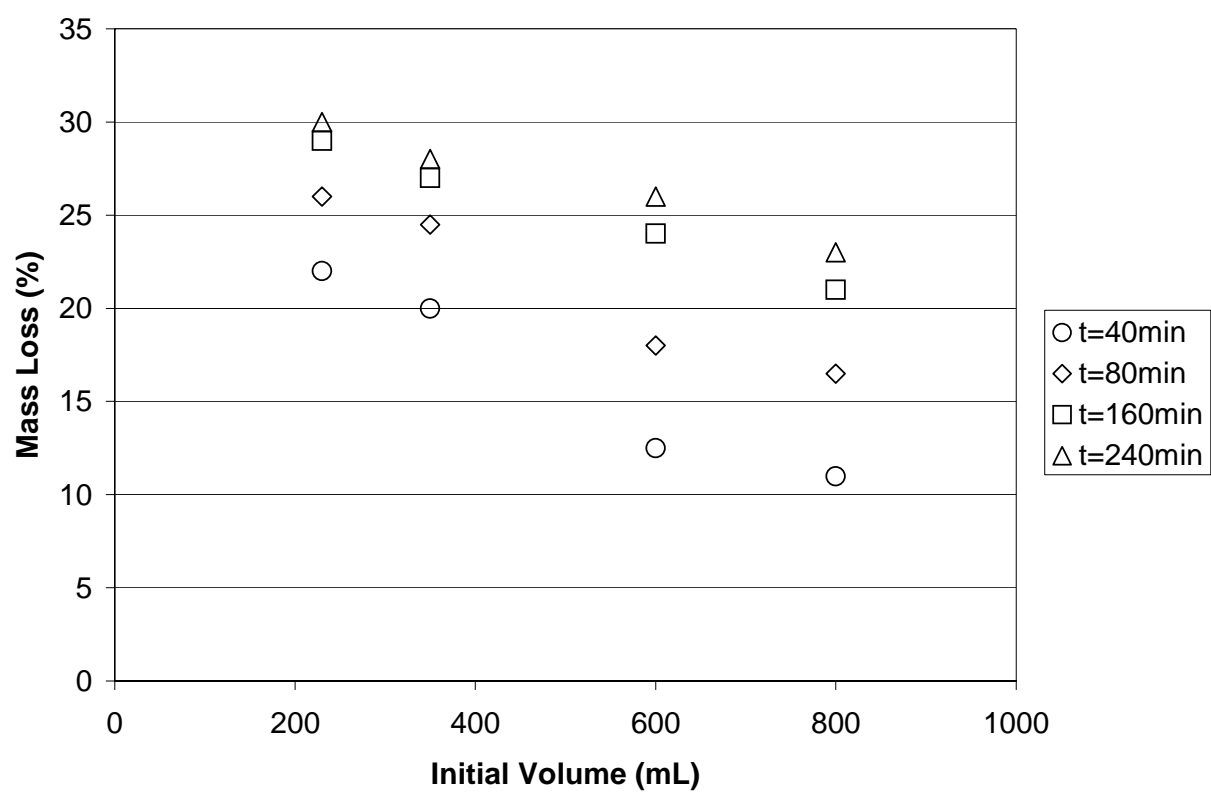
Wu et al.
Figure 2



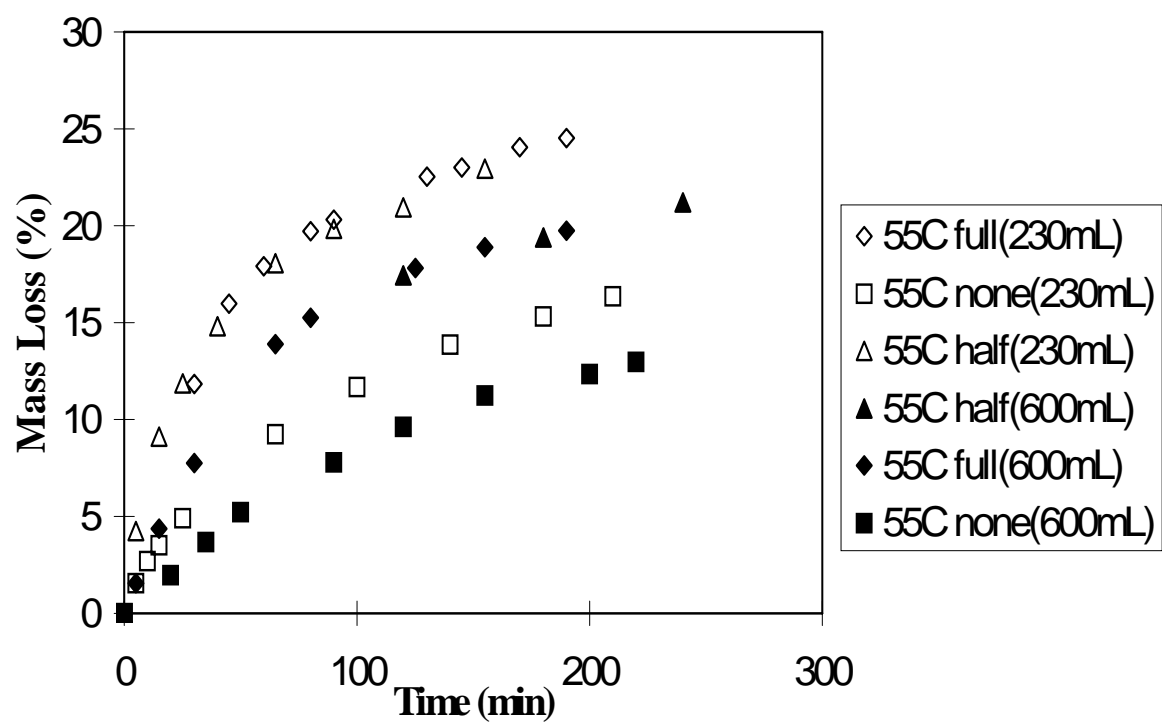
Wu et al.
Figure 3



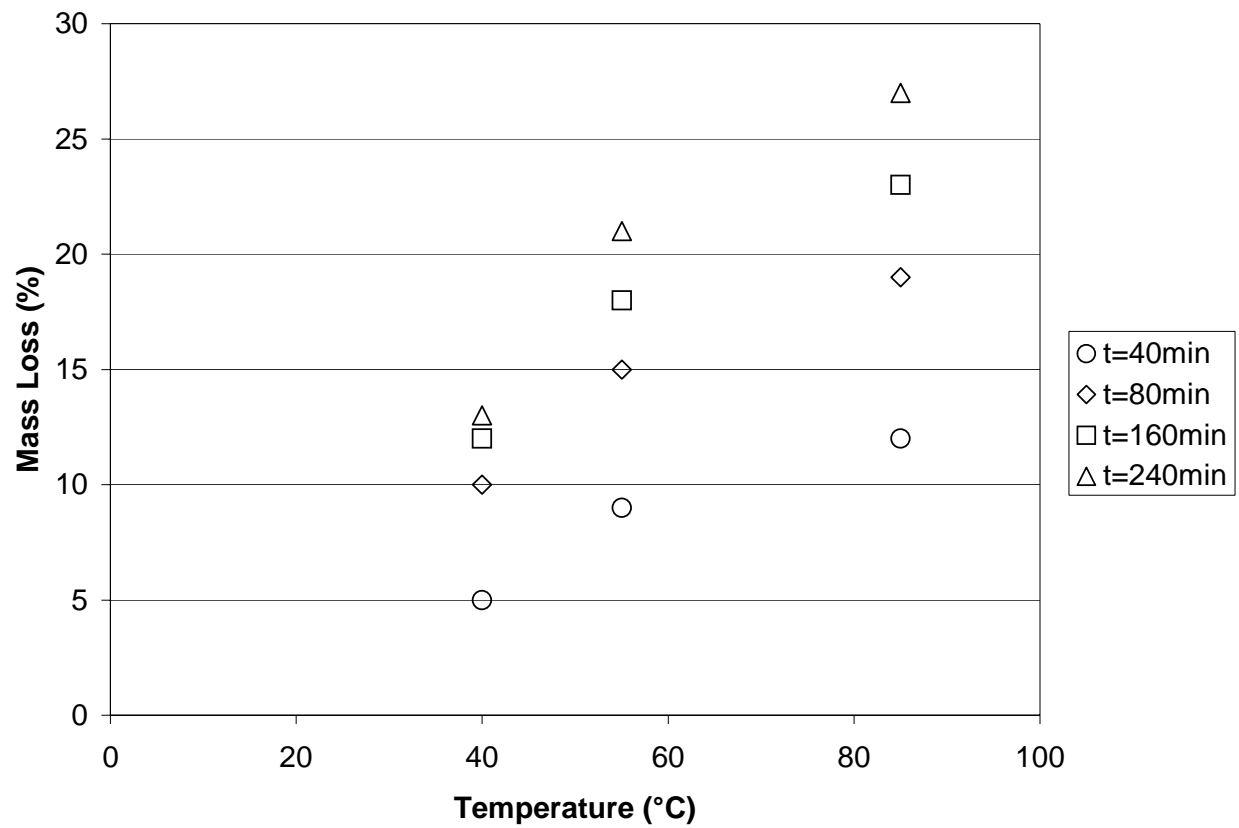
Wu et al.
Figure 4



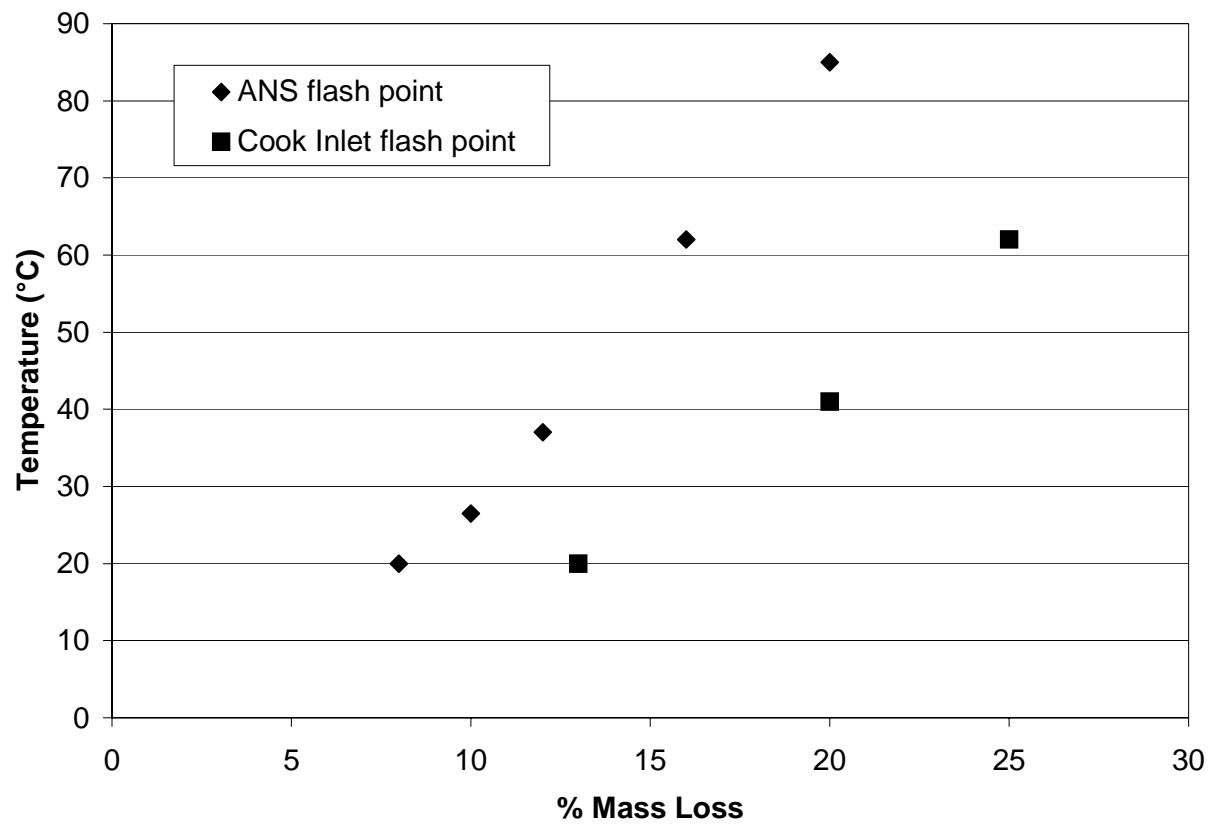
Wu et al.
Figure 5



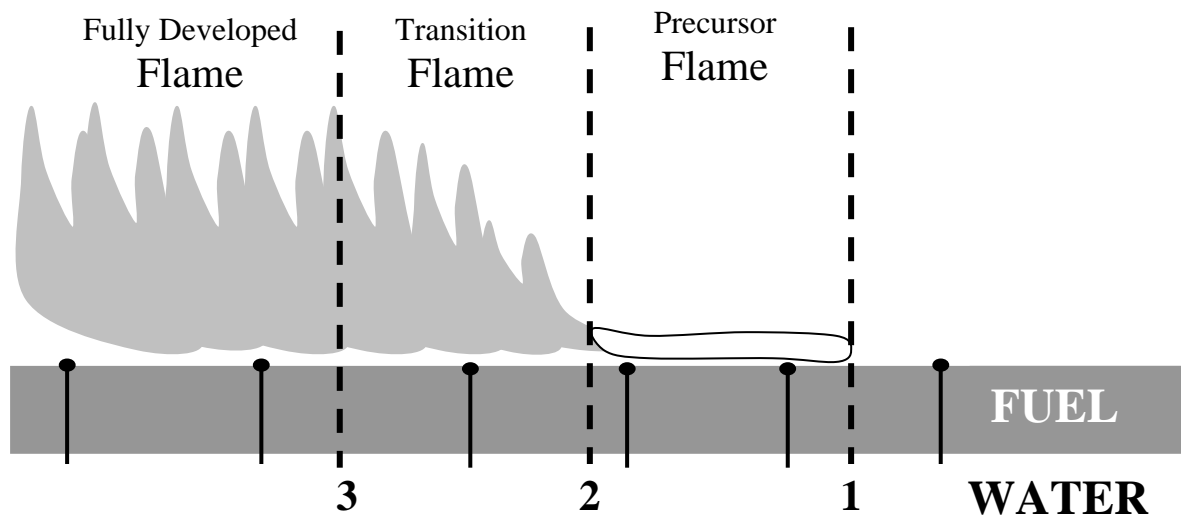
Wu et al.
Figure 6



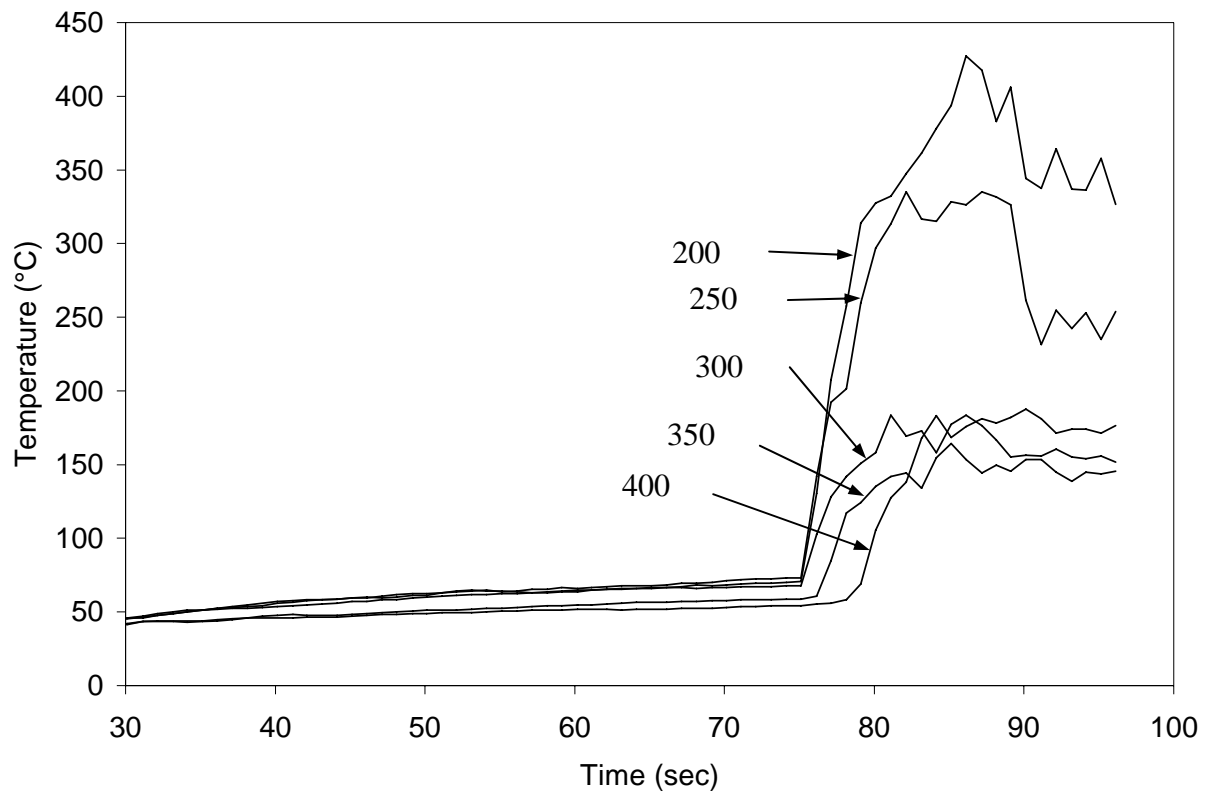
Wu et al.
Figure 7



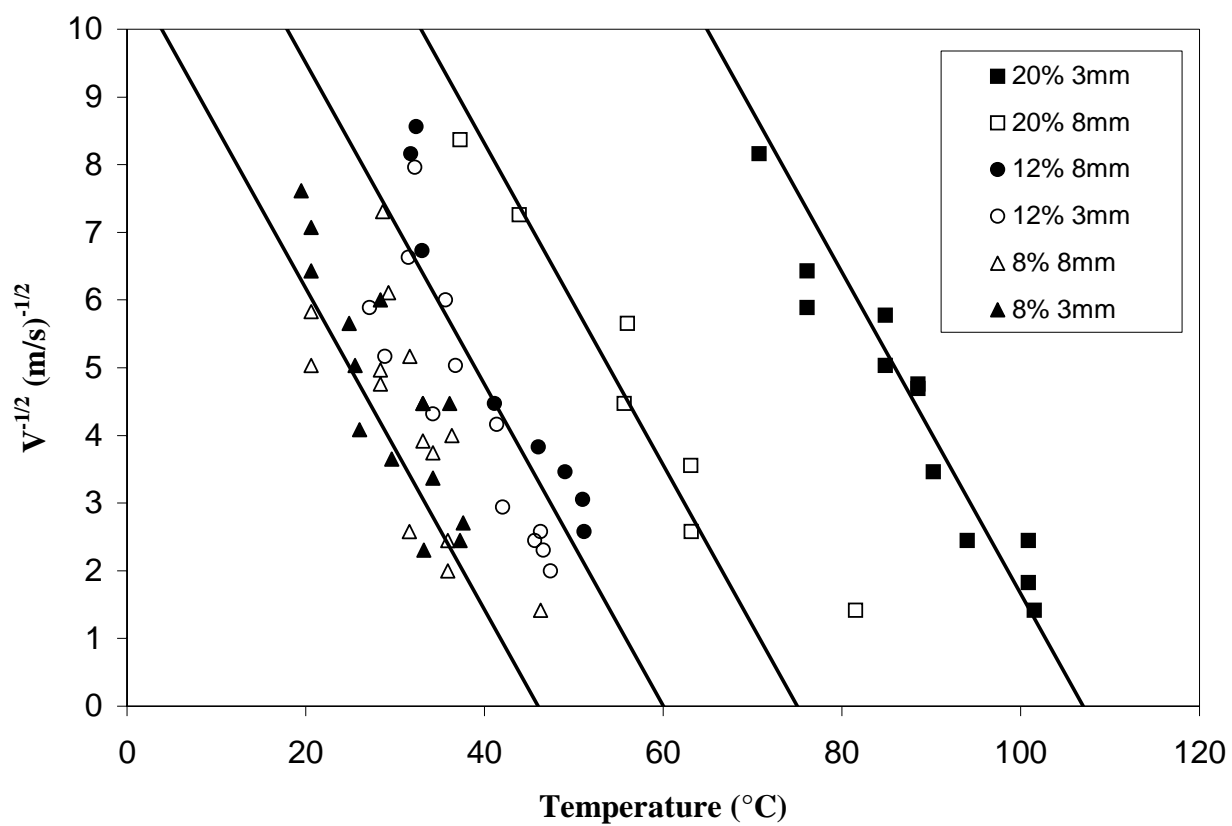
Wu et al.
Figure 8



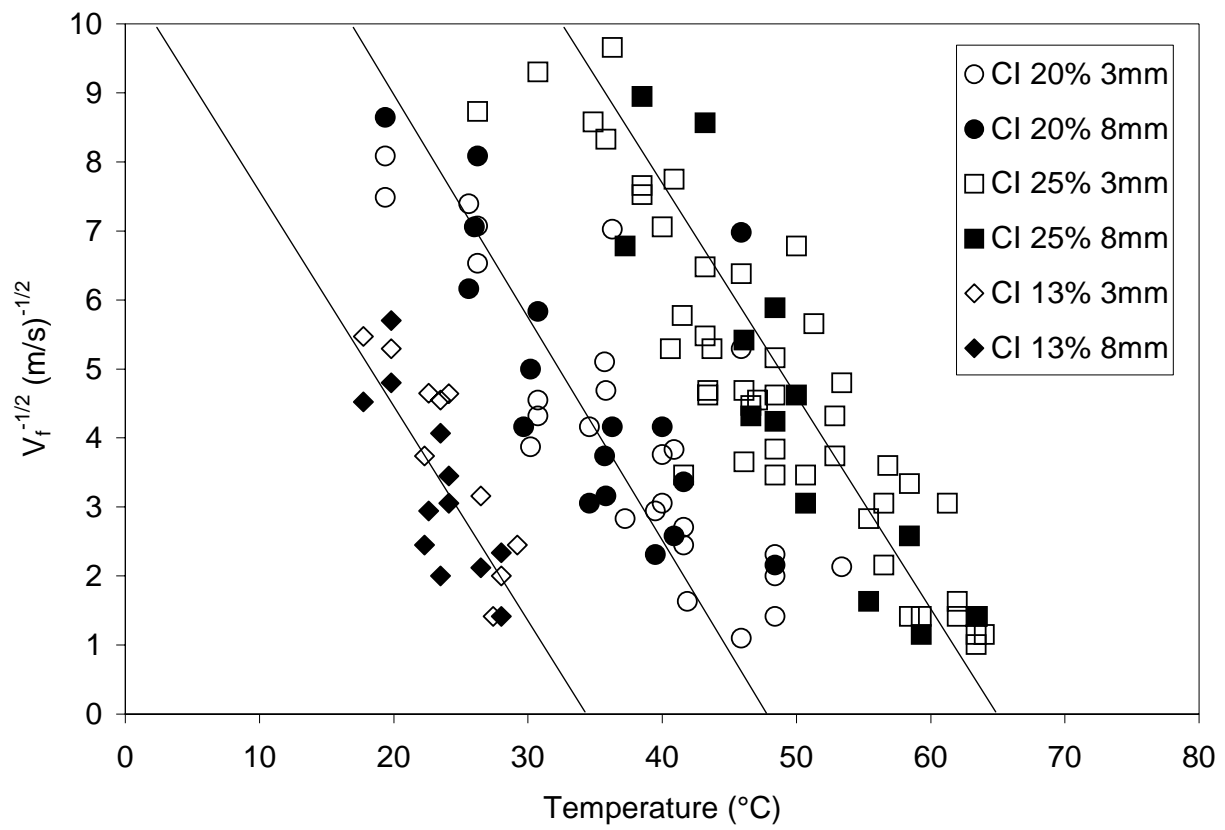
Wu et al.
Figure 9



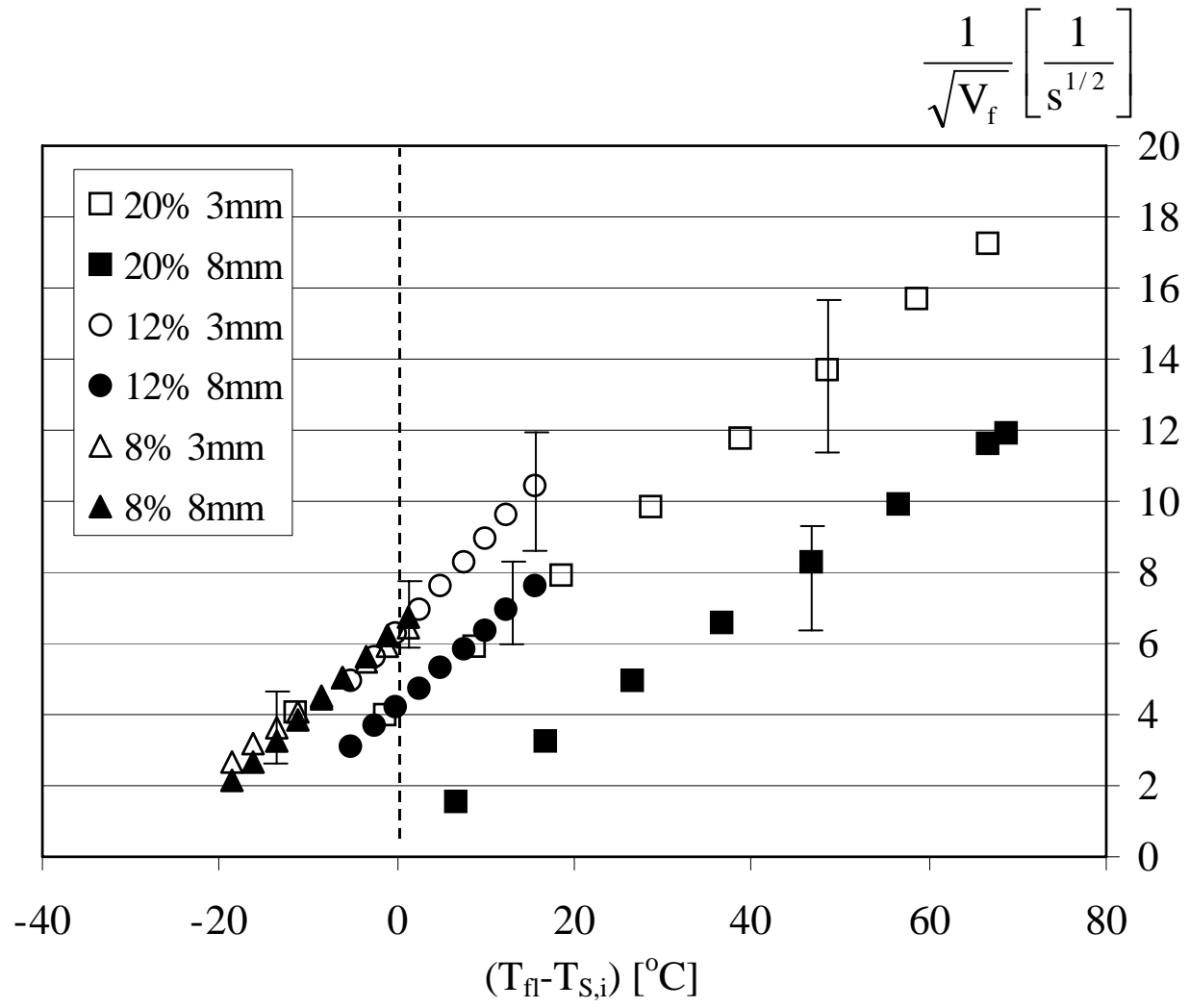
Wu et al.
Figure 10



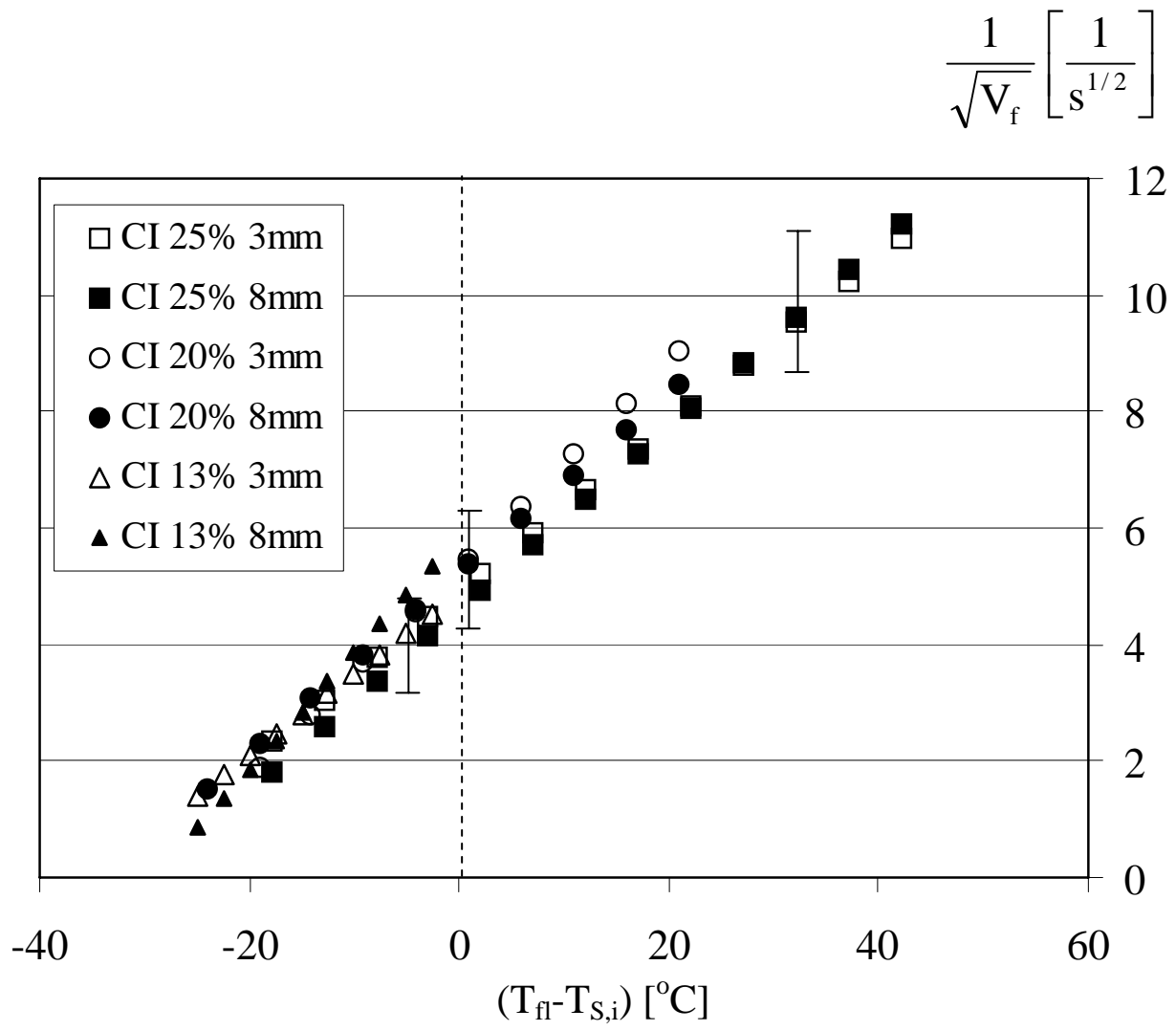
Wu et al.
Figure 11



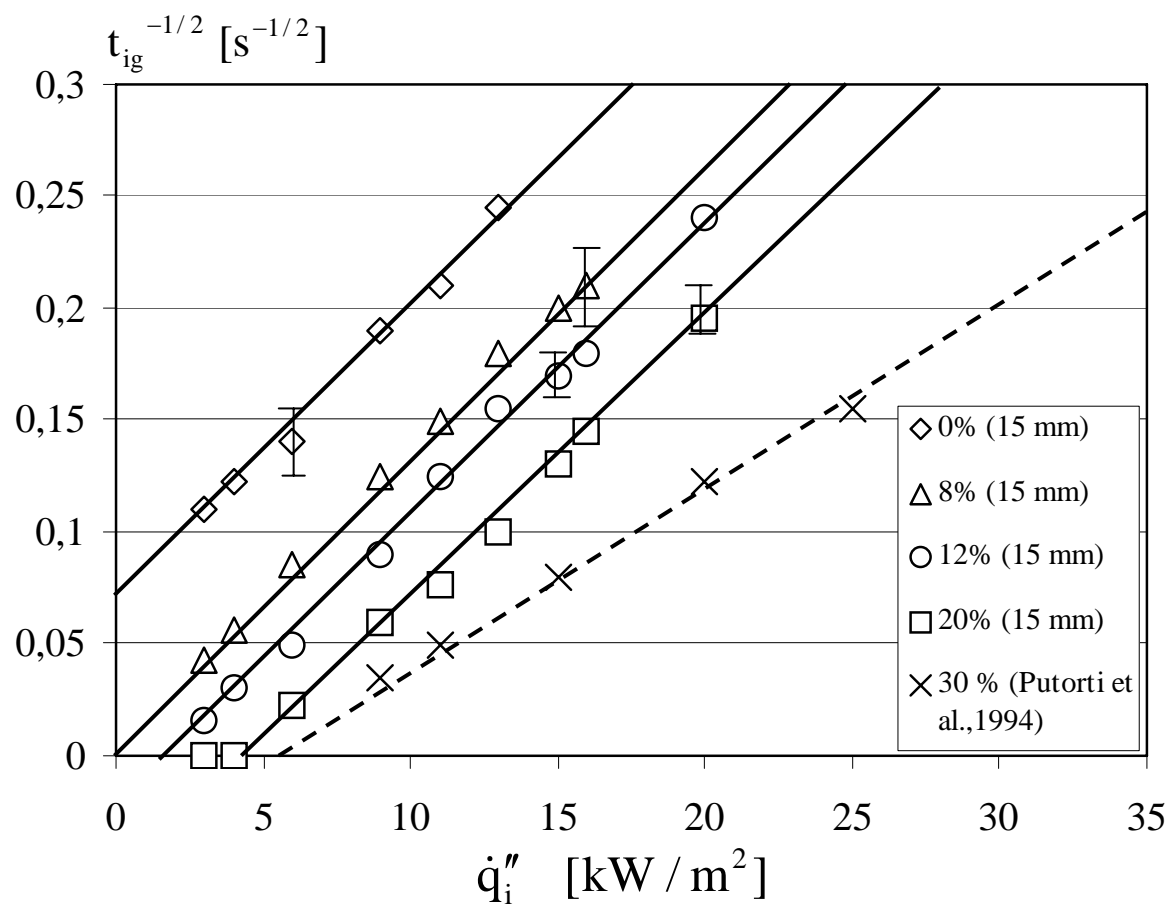
Wu et al.
Figure 12



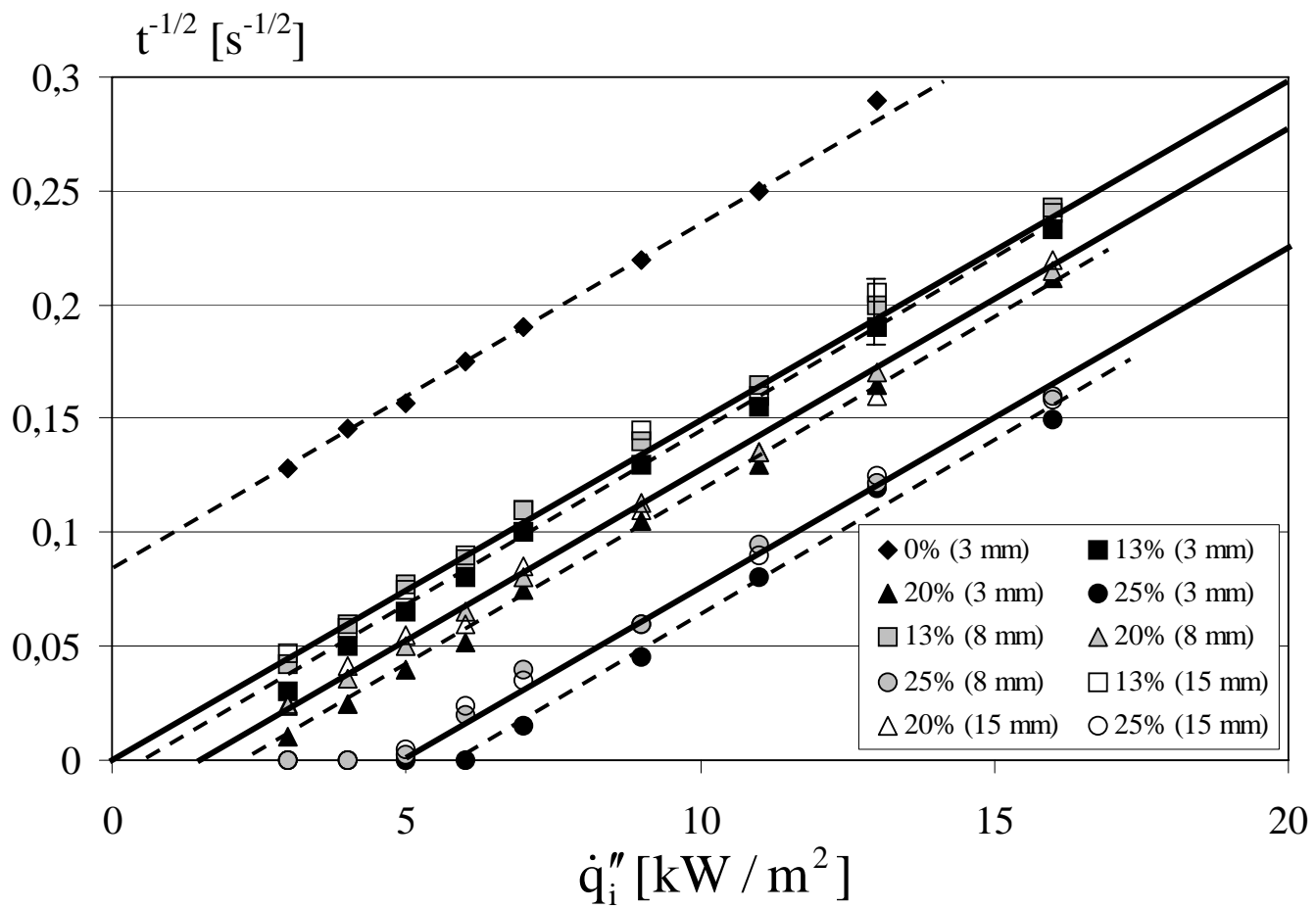
Wu et al.
 Figure 13



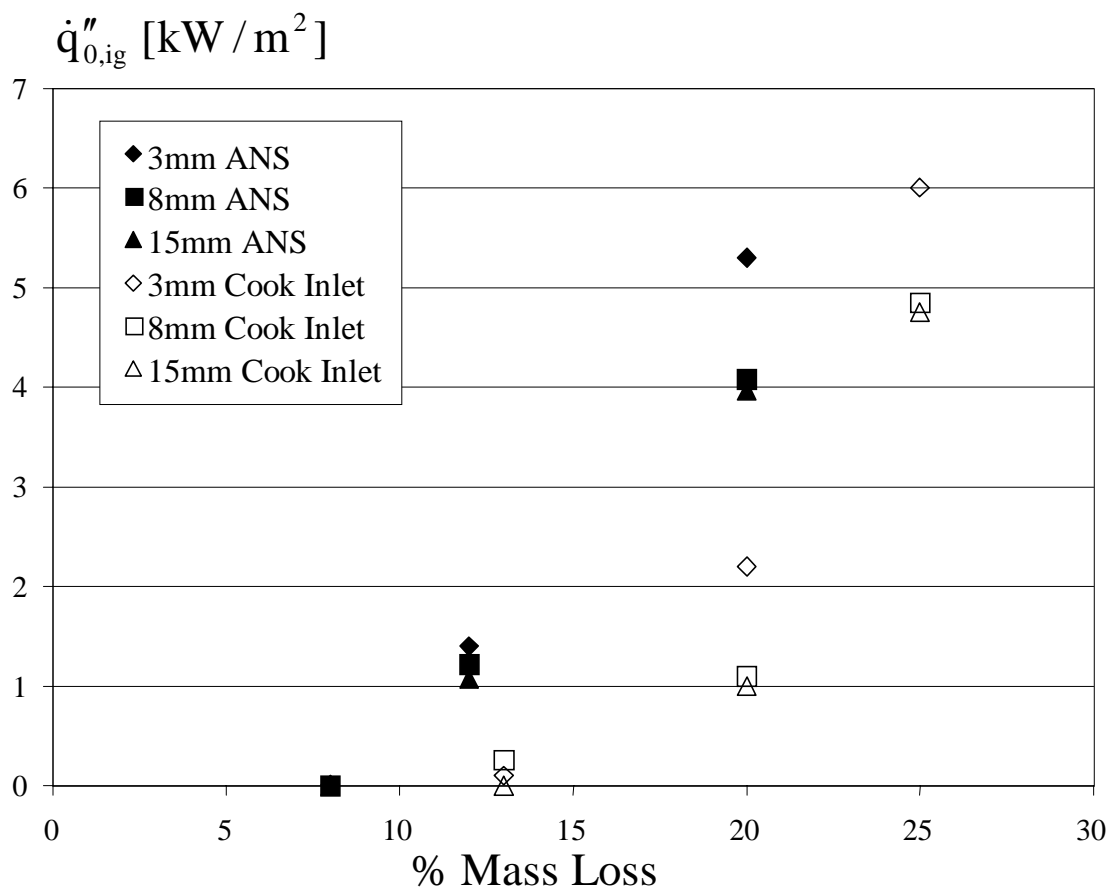
Wu et al.
Figure 14



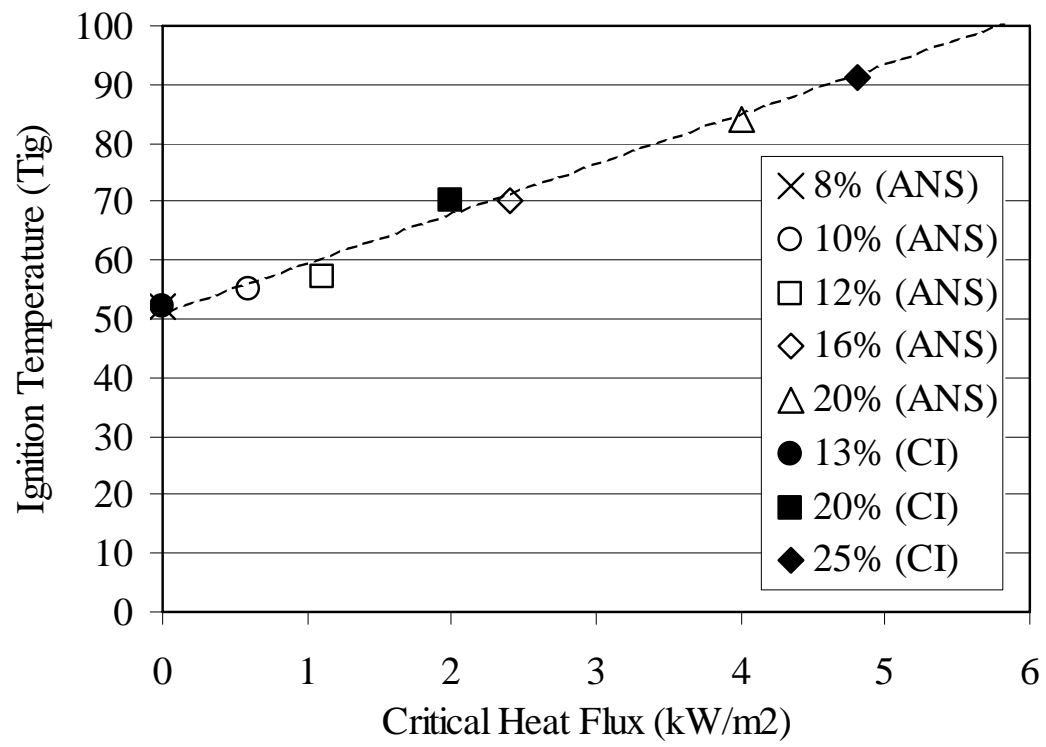
Wu et al.
Figure 15



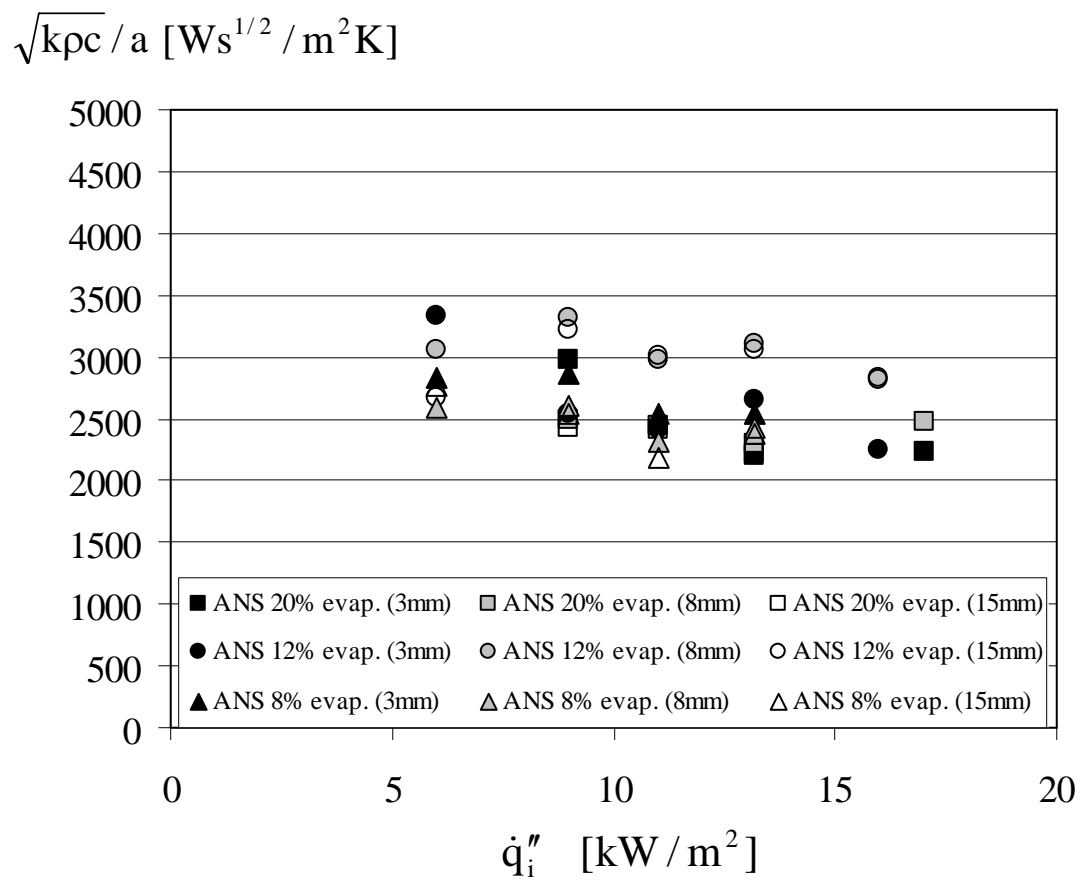
Wu et al.
Figure 16



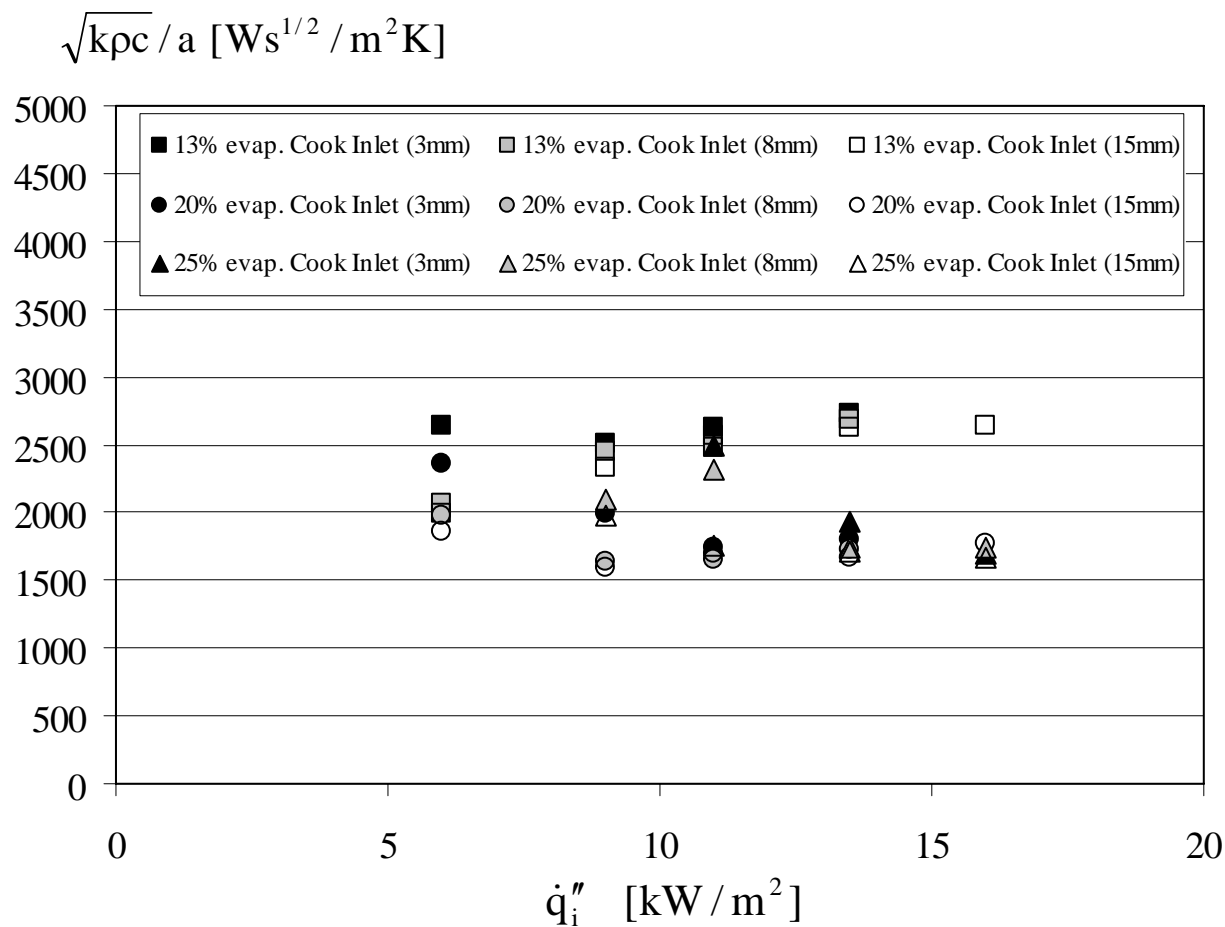
Wu et al.
Figure 17



Wu et al.
Figure 18



Wu et al.
Figure 19



Wu et al.
Figure 20